THE UNIVERSITY OF SYDNEY

Effects of Cusp Inclination and Occlusal Table Dimensions on the Loading on Implant Systems and Simulated Bone

by

Pimduen Rungsiyakull

A thesis submitted for the degree of

Master of Dental Science (Prosthodontics)

Faculty of Dentistry

The University of Sydney

29 August, 2008

DECLARATION

I hereby declare that the work described herein is, to the best of my knowledge, original and is entirely the work of the author, except where due acknowledgements have been made. The work was conducted while the author was pursuing a Master's degree program in Prosthodontics in the Faculty of Dentistry, the University of Sydney, under the supervision of Professor Iven Klineberg and Professor Mike Swain. I certify that this thesis has not already been submitted, wholly or in part, for the award of a higher degree to any other university or institution, that all help received in preparing this thesis, and all sources used have been acknowledged.

(Pimduen Rungsiyakull)

February 28, 2008

ABSTRACT

Occlusal surface design is an important factor for controlling force magnitude and direction on implant components and supporting bone. It has been recommended that reducing cuspal inclination and occlusal table dimension is beneficial to the long-term success of the implants and bone. The appropriate superstructure design, including the occlusal surface design of cuspal inclination and the occlusal table dimensions in single-implant restorations, needs to be investigated in an attempt to understand this influence on occlusal load and bone.

This study demonstrates a method to apply quantified axial forces to the four different occlusal design models – model one (30-degree cusp inclination with 6-mm occlusal table dimension), model two (30-degree cusp inclination with 3-mm occlusal table dimension), model three (10-degree cusp inclination with 6-mm occlusal table dimension), and model four (10-degree cusp inclination with 3-mm occlusal table dimension) by using an Instron universal testing system to simulate implant-supported single crowns and the supporting bone. Static loads from 50 N to 250 N were applied for 15 seconds and recorded. The applied forces were loaded on two loading sites; the central area and 2 mm buccally of the occlusal inclined plane. Data were analysed to compare the maximum principal strains (microstrains) registered by strain gauges in the buccal and lingual areas of the bone simulated model.

This study has shown that there are differences between the four occlusal design models. Loading on the central area of the occlusal specimens caused a significant difference in mean maximum principal strains compared with the 2-mm buccal loading of the occlusal specimens. Under loading applied at 2 mm, the highest mean maximum principal strain was seen in the model one, followed by model three and two. The lowest was presented in model four. Univariate Analysis of Variance (ANOVA) with post hoc test comparing the maximum principal strains (microstrains) for four different occlusal design specimens indicated a significant difference of the maximum principal strains (microstrains) between model one, two, three, and four, when an applied axial loading at 2 mm buccal on the inclined plane with strain gauges attached on the bone simulated model ($p = 0.000$).

The results from this study suggest that cusp inclination and occlusal table dimension significantly affect the magnitude of forces transmitted to implant-supported prostheses, which would have an effect on surrounding bone strains of dental implants when occlusal loads are applied in the clinical situations. The occlusal table dimension seems to play a more important role than cusp inclination, although the cusp inclination is still a factor to be considered. Moreover, combination of the two factors, cusp inclination and occlusal table dimension, significantly affects the magnitude of forces transmitted to implant-supported prostheses.

ACKNOWLEDGEMENTS

This thesis would not have been possible without the following people. I would like to express my deep and sincere gratitude to everyone who has helped and encouraged me, with special thanks to:

Professor Iven Klineberg, my supervisor, for his detailed and constructive comments, and for his important support and supervision throughout my Master's degree, both in clinical and research field. Thank you for giving me a great opportunity to be part of the prosthodontics program in The University of Sydney.

Professor Mike Swain, Head of the Biomaterial Research Unit, for giving me the great opportunity to be part of the Biomaterial Research Unit. His warm kindness and generosity have been a great support and inspiration for me.

Chaiy Rungsiyakull, my husband, to whom I also owe my most sincere gratitude for my thesis accomplishment. Thank you very much for all of your support in the Finite Element Analysis and experiments, your valuable time and friendly untiring help during my difficult moments.

Dr Richard Appleyard, for all the support and detailed advice since my first step in setting up the experiment with the Instron testing machine and strain gauges during the experiments.

Mr Ken Tyler, for his expertise and guidance on the technical work involved in the experiments.

Ms Terry Whittle, for her expertise and excellent guidance in statistical analyses.

My parents, my husband and my friends for all their loving and unremitting support in all ways. Without their encouragement and understanding it would have been impossible for me to complete my studies.

Nobel Biocare Australia for providing the implant fixtures and abutments used in the reseach project.

The Royal Thai Government Scholarship from the Royal Thai Government for financial support and giving me an opportunity to pursue a Master of Dental Science (Prosthodontics) at the University of Sydney, Australia.

TABLE OF CONTENTS

LISTS OF FIGURES

LIST OF TABLES

ABBREVIATIONS

B-L	Bucco-lingual
Fig.	Figure
FPDs	Fixed dental prostheses
SCs	Single crowns

CHAPTER 1

REVIEW OF LITERATURE

1. INTRODUCTION

Osseointegrated dental implants are accepted as clinically desirable and have predictable outcomes for the management of partially and fully edentulous patients. However, implant failures are still reported. Overloading and poor bone quality at the implant site are significant factors related to implant failures. Better answers are needed on whether successful implant-supported restorations are related to implant superstructure design.

The appropriate superstructure design; including occlusal surface design of cuspal inclination and the occlusal table dimension in single-, two-unit and three-unit implant restorations, need to be investigated in an attempt to understand the influence on occlusal load and bone.

2. IMPLANT SURVIVAL

In 1969, Brånemark and colleagues published research documenting the successful outcome of endosseous dental implant treatment (Brånemark et al., 1969). Since then, dental implants have had a profound influence on dentistry.

Complications with implants may be biological or technical (mechanical). Biological complications refer to disturbances in implant function by biological processes that affect the tissues supporting the implant, technical complications involve mechanical damage of the implant/implant components and suprastructure.

Complications reported include: implant loss, sensory disturbance, soft tissue complications, peri-implantitis, bone loss ≥ 2.5 mm, implant fracture and technical complications related to implant components and suprastructures (Berglundh et al., 2002).

Higher risks also exist for implants placed in compromised cortical (thin) and trabecular porous bone (type IV). Due to the poor structure of alveolar bone in the maxilla, dental implants have a lower survival rate in the posterior maxilla (Lindh et al., 1998).

A poor occlusion on implant-supported prostheses may affect supporting bone and prosthesis components. Studies have shown the consequences of

overloading of implants to result in loosening and fracture of components (Taylor and Agar, 2002; Walton and MacEntee, 1994).

There are several published systematic reviews and observational studies on the survival and success rates of implant-supported single crowns (SCs) and fixed dental prostheses (FDPs) in different modalities.

Naert et al. (2001a and 2001b) reported clinical studies of a total of 123 patients with 140 tooth-implant connected prostheses. The age of the patients at prosthesis installation ranged from 20 to 79 years (mean 51.8); 339 (BrånemarkA system) implants were connected to 313 teeth, and the loading time ranged from 1.5 to 15 years (mean: 6.5). They found more marginal bone loss (0.7 mm) for rigid and multi-connected tooth-implant connected prostheses compared to non-rigid connected tooth-implant. This suggests that bending load, which is increased in tooth-implant connected prostheses, might be responsible for this phenomenon. Moreover, tooth intrusion was found in the non-rigid connected tooth-implant prostheses in 34% of the cases. These observations favor the use of freestanding prostheses whenever possible.

Salinas and Eckert (2007) completed a systematic review to determine the long-term survival characteristics of implant-supported single crowns and tooth-supported fixed dental prostheses. The inclusion criteria included a minimum two-year study, published in the English language, and a minimum of 12 implants. From the outcomes, the authors failed to demonstrate any

direct comparative studies assessing the clinical performance of single-supported crowns and tooth-supported fixed dental prostheses. The pooled success of single-implant restorations at 60 months was 95.1% (CI: 92.2%-98.0%), while fixed dental prostheses of all designs showed an 84.0% success rate (CI: 79.1%-88.9%) (Salinas and Eckert, 2007).

Iqbal and Kim (2007) performed a systematic review to determine the outcomes of restored endodontically treated teeth compared to implant-supported restorations. Only 13 studies fulfilled the inclusion criteria. Data from the study indicated that there were no significant differences in survival between restored root canal-treated teeth and implant-supported single crowns.

Pjetursson and colleagues (2007) published a systematic review to analyse the survival and success rates by different types of tooth- and implant-supported fixed reconstructions and to evaluate the incidence of complications. They defined the term “survival” as a reconstruction remaining *in situ* with or without modification. The systematic review focused only on tooth- and/or implant-supported fixed dental prostheses and on implant-supported single crowns. They concluded that the estimated 10-year overall survival rates of the following three treatment modalities for the replacement of missing teeth were similar: tooth-supported conventional fixed dental prostheses (89.2%), implant-supported fixed dental prostheses (86.7%), implant-supported single crown (89.4%). Compared with tooth-supported fixed dental prostheses, the incidence of technical complications

was significantly higher for the implant-supported reconstructions. The most frequent technical complications were fractures of the veneer material (ceramic fractures or chipping), abutment or screw loosening and loss of retention (Pjetursson et al., 2007a).

3. BONE CONDITION AND IMPLANT OUTCOMES

Implant survival is dependent on the volume and quality of bone in the region of implant placement. Bone tissue is organised macroscopically into cortical and trabeculae structures. Cortical (compact) bone forms a dense surface layer, whereas trabeculae (spongy or cancellous) bone forms a three-dimensional network below the cortex (Robert and Arun, 1998).

In this review, the recommendations of Lekholm and Zarb (1985) and Norton and Gamble (2001) have been selected to classify jaw bone because they applied different techniques in classifying bone types.

Lekholm and Zarb (1985) developed a working classification of jaw bone condition to facilitate the planning of oral implants. They proposed a differentiation of jawbone quantity or shape (type A to E), and jawbone quality (types 1 to 4) in the anterior region of the jaws. This classification is as follows (Figure I -1):

Quantity (shape):

A. Unresorbed alveolar bone

B. Some resorption of alveolar bone

C. Complete resorption of alveolar bone

D. Some resorption of basal bone

E. Extreme resorption of basal bone

Quality

1. Primarily cortical bone
2. Thick cortex with dense cancellous bone
3. Thin cortex with dense cancellous bone
4. Thin cortex with low-density cancellous bone

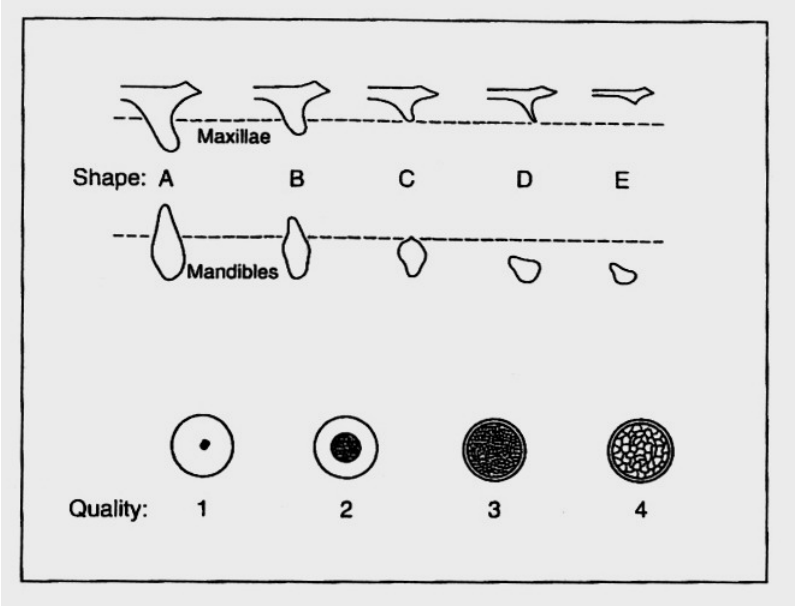

Figure I – 1 Classification of jaw bone by Lekholm and Zarb (1985)

Generally, the mechanical properties of bone are governed by its mineral content and structural composition, that is, the cortical/cancellous bone ratio

(Friberg et al., 1995). The maxillary cortex is substantially thinner and more porous than the mandibular cortex. Thinner trabeculae and lower trabecular bone density have been found in posterior compared with anterior jaw sites, and in the maxilla compared with the mandible (Ulm et al., 1992). The bone site is related significantly to osseointegration potential, and mandibular sites have proven to be more successful than maxillary sites. The responses of trabecular bone to the mechanical environment are a critical factor, especially in the posterior maxilla, where cortical thickness and properties of trabecular bone may be insufficient to withstand occlusal forces.

Bone typing is useful at all stages of treatment planning and case management. The pre-operative identification of a particular bone type can influence the choice of implant surface, the anticipated dominant mechanism of endosseous integration, and the loading protocol. However, there is a lack of evidence to support the validity and reliability of methods used to assess jawbone condition pre-operatively (Bryant, 1998).

Methods to evaluate bone quality and quantity have relied on generalised clinical criteria (clinical assessment), radiographic/imaging techniques, and surgical assessment at the time of the osteotomy. Computerised axial tomography (CT) is an established method for acquiring bone images before implant placement. Quantitative cone-beam computerised tomography is preferred method, particularly as the associated radiation dosage is reportedly much lower (Aranyarachkul, 2005).

In recent years, micro-computed tomography (micro-CT) technology has become popular and has enabled the determination of cancellous bone microstructure with greater accuracy. However, the most recent study is of human cadavers (Aranyarachkul, 2005), and few data are available on this topic. One in-vivo study, which aimed to develop a new x-ray microtomography technique to determine the structure of bone surrounding implants, studied samples from retrieved micro-implants. However, the study used few samples and requires evaluation of the accuracy of the technique (Sennerby et al., 2001).

4. BIOMECHANICAL AND OCCLUSAL CONSIDERATIONS

4.1 LOADING ON IMPLANTS

The peripheral neural feedback system with implants is different from that of teeth, as a result of the absence of the periodontium and the mechanoreceptors located in periodontal tissues. However, there are other peripheral mechanisms and also central neural changes in response to the feedback (Klineberg et al., 2007).

In general, functional loading is transient except in situations that need higher loads, such as tough food. Thus, the load points or areas of loading are important and loads should ideally be directed along the long-axis of the crown and implant.

Heitz-Mayfield et al. (2004) reported on an experimental study in the dog and concluded that loading is a trigger for bone remodelling, and that transient loads, which are within normal function, appear to be acceptable physiologically.

Stanford (2005) reviewed the literature on the issue of implant occlusion and stated that the adaptive capacity of bone for dynamic growth (modelling) and remodelling allows the implant interface in general to withstand and adapt to varying occlusal loads in function and parafunction.

The optimal transfer of vertical occlusal load through an implant is along the long-axis. This is not always achievable, due to anatomic features. Alignment of the occlusal load in a direction different from the vertical force, that is, as an “offset” load, will lead to bending moments created within the implant. Other influences on the implant, even if load is primarily axially aligned, include lateral forces and prosthetic cantilevers.

Balshi (1996) reported that patients with parafunctional habits were especially susceptible to implant bending moments in the posterior region. Bending moments lead to higher stress levels in the implant components and the supporting bone than those caused by compressive or tensile forces, and can lead to bone loss and implant fracture (Rangert et al., 1995; Balshi, 1996).

Overload of implant prostheses is one of the factors contributing to implant failure. Overload is a fatigue phenomenon and may lead to various types of mechanical failure from accelerated wear, such as chipping and fracture of porcelain and abrasion of acrylic resin, to overt screw loosening, and fracture of abutments or even implants (Schwarz, 2000). Moreover, it needs to be addressed that occlusal overload can cause biological complications such as peri-implant bone loss (Misch et al., 2005).

As described in the literature review by Brunski et al. (2000), in-vitro and clinical reports on mechanical issues have been restricted only to integration failures in the early healing phase related to micromotion and late failures by overload. Brunski and colleagues stated that features of overload include repeated screw-loosening, fracture and loss of crestal bone in cyclic loading conditions. Microdamage, which maybe induced from overload, may contribute to increased bone fragility and fracture risk. Fractures can develop as a result of a positive feedback cycle of damage. Porosity is induced by remodelling, which then further weakens the bone, leading to further damage. The authors cited animal experiments (Isidor, 1996, 1997), and computer simulations using finite element images, all of which implicated excessive loading as a cause of loss of implant integration and bone loss.

It has been stated in animal experimental studies that high cyclial loads have a more detrimental effect on the surrounding bone of dental implants than static loads. The study by Duyck et al.(2001) showed that excessive

cyclial loads can cause crater-like bone defects lateral to dental implants. After applied static and cyclial loads for 14 days to 10 mm long implants, inserted bicortically in rabbit tibiae, no histological change was seen in the control and statically loaded implants. Similar results were also observed in a series of dog experimental studies by Gotfredsen et al. (2001a-c and 2002) where no implant failure was found in the models loaded with static loads.

4.2 HUMAN MASTICATORY FORCES

Excessive loading of implant-supported restorations is reported to induce biological and technical complications, such as crestal bone resorption. Therefore, it is important to understand how much human masticatory force is generated on implant-supported restorations.

Brånemark et al. (1977) estimated average biting forces of 125 N with a maximum force of 400 N. It was not mentioned whether the forces were derived from anterior or posterior biting. The magnitude of biting force was a factor in the calculations for the necessary minimum strength of implant-to-bone contact. The study was limited to restorations of the edentulous mandible, and implants were only placed in the anterior mandible. However, these Figures should be presumed to reflect both anterior and posterior forces (Brånemark et al, 1977).

Richter (1995) reported on maximum vertical force levels of up to 121 N during the chewing cycle with different food textures on implants in the posterior region, and 30 N for transverse forces. Clenching alone without

food registered in the order of 50 N of vertical force. Factors influencing the magnitude of biting forces included dysgnathia (dolichocephalic lower than brachiocephalic), gender (females lower than males) and degree of edentulism. The author used a transducer measuring device as a substitute for the internal abutment complex of the implant restoration to measure the physiological levels of bite force on implants. Other findings included the maximum bite force on teeth with crowns (150 N), and mean maximum biting force for both teeth and implants (< 80 N each) (Richter, 1995).

In their review, Brunski et al. (2000) cited several studies on bite forces after implant treatment. They reported that mean maximum forces varied from 112.5 N to 450 N. One study registered a maximum bite force of 1,100 N in one subject. Data from studies of bite force in the optimum dentition were in general reported to be in the range of 469 N (canine) to 723 N (second molar), with lateral bite forces estimated at 20 N.

Bite force is also associated with food consistency. Wang and Stohler (1990) studied different textures of food, i.e. carrot, beefstick, peanut and monkey chow to measure the breaking force of different foods of standardized size and shape with a universal testing machine. They found that each test food has specific properties reflected in characteristic details of its force-time curves, and that reproducibility decreases with increasing hardness of the material under the loading test.

The reporting of data in the literature on bite force needs to be qualified by variables including antero-posterior location, dysgnathia, gender, relative edentulism, measurement technique, and force vector resolution.

Human masticatory forces have been studied by various means, although range of magnitude of forces can be accepted, notwithstanding the methodological and subject variations.

The magnitudes of human masticatory forces are useful when evaluating desirable material properties such as fracture toughness and flexural strength, or limiting restorative strategies such as occlusal scheme design and cantilever length.

4.3 IMPLANT BIOMECHANICS

The relationship of the applied load from the prosthesis with the supporting capacity of implant and bone will affect the long-term outcome of treatment.

There are many possible factors involved in controlling the load level of a restoration, such as, implant number, implant position, implant angulation, leverage, bone support, force generation, occlusal design and occlusal contacts.

Implant angulation resulting from placement restricted by anatomical boundaries such as the posterior mandible, where implant placement is restricted by the inferior alveolar canal and its neurovascular contents, the

floor of the mouth and the resorbed crestal bony ridge are factors which may induce non-axial loading. Taylor et al. (2000) advised that avoidance of non-axial loading of dental implants is a clinical concern not based on scientific evidence. The concern is justified, however, when the issue is extended to include the restorative components, for example, screw-retained components, interface tolerances, plastic deformation, wear and fatigue failure.

The number of implants, distribution and splinting of implants are issues that involve not only implant biomechanics and anatomical limits, but also potential cost savings for the patient. Taylor et al. (2000) stated that restorations designed, according to both extremes, for example, full-arch prosthesis on four implants, or one implant per missing tooth, can be shown to be successful in a given clinical situation.

Rangert et al. (1997) defined this issue under geometric load factors. Their work was modelled by evolving a theory based on engineering principles, an analysis of complications such as fractured implants, then a revision of theory. They emphasised the importance of cross-arch stabilisation for full-arch restorations, which allows fewer implants per prosthetic unit. Their explanation was that implants in a complete-arch restoration may be considered as strategically placed prosthetic supports, so that axial implant forces across the arch counteract lateral contacts. Implants in a short-span posterior prosthesis function to a higher degree as tooth root substitutes, because they will gain less support from each other. They described the

concept of "support value", where in each tooth root represents one support. If the lost support value, SV, is three or less, then the number of implants ideally should be equal to the SV. That is, if the number of implants is less than the support value when the SV is less than or equal to three, a load factor risk is present. For larger restorations, three implants represent the minimum number, because strategically curved placement mimics the cross-arch stabilization effect in full-arch prostheses. That is, where less than three implants support a restoration of four lost support values, a load factor risk is present.

In the situation of inadequate space for implant placement, for example, a single molar pontic space is typically too narrow for a wide implant plus another regular or wide implant. Bahat and Handelsman (1996), in an earlier clinical report found failure rates of 1.6% and 3.4% for paired - any combination of 3.75 / 4 / 5 mmØ - unpaired 5 mmØ over a mean post-loading period of three years in the posterior jaw. They stated that it will be necessary to compare the long-term effectiveness of single standard and wide implants as well as double implants (Bahat and Handelsman, 1996).

Tripodisation, or an offset of 2-3 mm between implants, can reduce the bending moment of a three-implant restoration by 20-60% (Rangert et al., 1997). Implants which are placed in line have a rotational axis; this configuration presents a load factor risk. Taylor et al. (2000) supported the geometric principle of tripodisation. However, this concept has been cautioned against, as it has not been prospectively demonstrated clinically

to be superior to a more conventional two implants supporting fixed dental prostheses.

Cantilevers appear to have greater impact both in the partially edentulous situation and in full-arch situations. In principle, cantilevers should not be accepted as a routine arrangement on posterior partial prostheses in the same way as for full-arch. Cantilevers, bucco-lingual offset of the restoration, and excessive height of the abutment-crown complex with lateral forces will each increase the stress on the implants.

In-vitro studies have shown that the effect of splinting implant crowns reduces peri-implant bone stress (Wang et al., 2002) and improves load-sharing by eliminating the risk of excessive non-passive situations from excessive contact tightness that would be present in situations between individual crowns (Guichet et al., 2002).

4.4 OCCLUSAL SCHEMES

Occlusion is an important factor for controlling force magnitude and direction. If cusp inclination is increased, this situation can create the leverage and, as well, the more lateral the tooth cusp the greater contact leverage will result. By centering the occlusion and reducing the occlusal table, the lever arm will be reduced. A careful consideration of the design of occlusal surfaces and the cusp contact pattern is an important tool for limiting the stress on implant and bone (Rangert et al., 1995, 1997).

4.4.1 OCCLUSAL DESIGN

The concept of posterior occlusal forms and posterior tooth arrangements has been proposed since the early twentieth century for removable prostheses. Terms describing occlusal features for posterior tooth form and arrangement, and for lateral tooth guidance include (Klineberg et al., 2007):

1. Posterior tooth form (tooth inclination)
    a. No cups or cuspless or 0^{o} teeth
    b. Monoplane teeth
    c. Cusped teeth 20^{o} and 30^{o}
2. Posterior tooth arrangement
    a. Balanced with cusped teeth
    b. Lingualised with modification of cusped teeth
    c. Cuspless arrangement
3. Tooth guidance
    a. Canine guidance
    b. Group function

Decreasing the size of the occlusal table by reducing the number of teeth and/or reducing the bucco-lingual or bucco-palatal width is another specific occlusal design feature proposed by Christensen (1962) to reduce torque forces on the distal abutment in removable and fixed dental prostheses.

4.4.2 OCCLUSAL DESIGN IN IMPLANTS

Dental implant occlusion has characteristics following the natural and restored dentition, which are developed from removable prosthodontic concepts. The aims in designing an implant occlusion are to (Hobkirk,

2004): maximise occlusal function, minimize harm to opposing and adjacent teeth, minimize the wear on occlusal surfaces, minimise the risk of fracture of the implant superstructures and reduce the risk of fracture of the implant and its connecting components.

4.4.2.1 OCCLUSAL MATERIAL

The preferred material for the occlusal surface of implant superstructures is still equivocal. The original recommendations for resinous materials in full-arch situations after osseointegration were introduced in 1982, instead of metallic and ceramic for fixed implant restorations. It was believed that the implants would be protected from functional and parafunctional loads and acrylic resin would cushion occlusal loads to benefit the osseointegrated interface. However, the effects of food consistency and individual variation in masticatory forces seem to play a more important role. Other factors also need to be considered, such as longevity, abrasion resistance, appearance, ease of fabrication and ease of repair.

During each period of implant use, treatments were typically fixed full-arch edentulous mandibular bridges opposing removable complete maxillary dentures. The emergence of single tooth and partially edentulous implant restorations, for which aesthetics and wear resistance were of greater concern, led to the use of porcelain materials. The use of acrylic for provisionalising in "progressive implant loading" treatments was recommended (Misch, 1999). The

standard of care for implant-supported restorations today includes the use of ceramic occlusal materials (Taylor et al., 2000).

Studies comparing the distribution of stress across fixed implant restorations, among gold, porcelain and resinous materials, have drawn varying biomechanical results and conclusions.

Cibirka et al. (1992) reported on an in-vitro simulation study using the strain gauge measurement. They compared the forces transmitted to human bone by gold, porcelain, and resin occlusal surfaces and found no statistically significant differences in the force absorption quotient of the occlusal surfaces among these three materials (Cibirka et al., 1992).

Weinberg (1998) found stress to be concentrated at the cortical bone around the cervical region of the implant, and that gold alloy and porcelain produced the highest stress values in this region, compared with resinous materials which registered values of 15-25% lower than the other materials.

4.4.2.2 OCCLUSAL SCHEMES

The effect of cantilevers, bucco-lingual offset and excessive crown-abutment heights as load factor risks have been discussed earlier (see Implant Biomechanics).

Research on the effects of occlusal design on the outcome of implant treatment is limited, so that a number of general principles are proposed on the basis of a small number of studies and limited clinical experience. Different ways to assure that the load is favourably distributed between implants and natural teeth are important to minimise the risk on the implants and supporting bone. If the component of lateral force is not controlled, this situation should be designated a load risk factor (Rangert, 1997).

Kaukinen et al. (1996) in an in-vitro study, reported on the influence of occlusal design (cusp inclination) on force transmission to a simulated implant-retained prosthesis and the bone supporting the implant. The baseline deflections registered by the strain gauges on the bone were analysed in relation to different food consistencies. They concluded that no significant differences were demonstrated in maximum breakage forces or maximum strains between the 33-degree cusped and the 0-degree cuspless occlusal design specimens. However, the initial breakage force for the 33-degree cusped occlusal design specimens was greater than the initial breakage force for the 0-degree cuspless occlusal design specimen.

Weinberg (1995 and 1998) described various means to assist in the reduction of torque from loading, such as reduction of cuspal and cingulum inclination, and relocating the occlusion to a cross-occlusion in the case of a lingually inclined maxillary molar implant. Of particular

interest was the description of a modified centric molar occlusal anatomy from the typical sharp-lined fossae to a 1.5-mm flattened horizontal fossa. The techniques were geometrically rationalised and practical guides utilising an articulator were described and detailed.

Recent reviews have suggested the desirability occlusal modifications aimed at reducing axial and/or lateral loads on dental prostheses. The application of biomechanical principles such as passive fit of the prosthesis, reducing cantilever length, narrowing the bucco-lingual and mesio-distal dimension of the prosthesis, reducing cusp inclination, eliminating or reducing excursive contacts on posterior segments, and centering occlusal contacts have been recognised as important (Kim et al., 2005; Stanford, 2005).

For the occlusion on posterior fixed prostheses, it has been suggested that anterior guidance in excursions and initial occlusal contact on the natural dentition be used, to reduce the potential lateral forces on osseointegrated implants. Group function occlusion should be utilised only when anterior teeth are periodontally compromised. Moreover, reduced inclination of tooth cusps, centrally oriented contacts with a 1-1.5 mm flat area, a narrowed occlusal table, and elimination of cantilevers, are key factors to reduce bending and overload in posterior restorations (Curtis et al., 2000). In this in-vivo study, it was reported that narrowing the bucco-lingual width of the occlusal surface by 30% and chewing soft food

significantly reduced bending moments on posterior three-unit fixed prostheses (Morneburg and Pröschel, 2003).

Klineberg et al. (2007), in a systematic review, reported on the basis for using a particular occlusal design in tooth and implant-borne reconstructions and complete dentures. Twenty-three articles met the inclusion criteria on implant superstructure design and data were extrapolated from studies with low levels of evidence up to low-level RCTs. They mentioned that there is little evidence to indicate that a particular occlusal design is superior. Guidelines (Klineberg et al., 2007) for occlusal scheme design with implants have been summarised in this study from the literature (Khamis et al, 1998; Duyck et al, 2000; Goodacre et al, 2003; Wood and Vermilyea, 2004; Kim et al., 2005; Stanford, 2005; Taylor et al., 2005), as followed:

- General features of occlusal form:
  - Reduced cuspal imclination
  - Wide grooves and fossae
  - Narrow occlusal table
  - Supporting cusps in central fossa to generate forces along the long-axis
- Occlusal scheme design:
  - Bilateral simultaneous contacts in centric relation and intercuspal position with 0.1-1.5 mm “freedom of centric”
  - Reduced cantilever length from distal implant

- Anterior guidance for smooth lateral movements without posterior tooth contact
- No contact on cantilever in intercuspal position, centric occlusion or lateral movements; shim stock (10 µm) clearance with clenching
- Lateral guidance as group function when opposing teeth and as lingualised occlusion when opposing complete dentures
- Single implant crowns – shim stock (10 µm) clearance at in intercuspal position and centric occlusion

Currently, there are little evidence-based design concepts for implant loading occlusion. Most of the studies are based on clinical opinion with little objective evidence to support proposed concepts. Further study needs to investigate the relationship between the occlusal design and implant longevity related to occlusal load and surrounding bone.

4.5 ROLE OF STRESS AND STRAIN IN RELATION TO BONE REMODELING AND OCCLUSAL DESIGN

It has been stated that occlusal forces affect the surrounding bone of dental implants and can result in loss of marginal bone or loss of osseointegration of dental implants (Naert et al., 2001a and Naert et al., 2001b).

Bone remodeling is defined as a process where bone changes its internal microstructure and external morphology in any form, size, or shape to adapt to the loading conditions. It is also a surface-specific phenomenon that occurs during growth as part of wound healing and in response to bone loading (Marx, 1998). Mechanical stress can have both positive and negative consequences for bone tissue (Frost, 2004). The longevity and stability of dental implants can be improved if a positive healing process occurs.

There are several factors causing loss of osseointegration, and the consequences of mechanical load is one of the important factors that needs to be considered. The bones of the maxilla and mandible, as well as other bones carrying mechanical loads, adapt their strength to the applied load (Forst, 1992; Forst, 2004 and Isidor, 2006). Mechanical stress on bone results in strain, which is defined as the relative change in the length of the bone. This is always expressed in microstrain units, where 1,000 microstrains correspond to a deformation of 0.1%. The strain is dependent on the mechanical properties of the materials, so that the applied force may affect different bone or bone tissue differently. That means that the same amount of stress can result in different amounts of strain in bones with different properties.

Isidor (2006) reviewed 607 papers on forces on peri-implant bone. The author reported that bone is believed to function within the strain range of approximately 50 – 1500 microstrains (Frost, 2004). If the peak load on bone results in strains of 1500 – 3000 microstrains, a mild overload occurs

and compensates by gaining more bone. If the strains exceeds a threshold, i.e. more than 25,000 microstrains, bone fracture can suddenly occur, leading to a negative remodeling and bone loss. On the other hand, if the bone strain does not exceed 50–100 microstrains, bone is not stimulated, leading to a net loss of bone. Optimal functional strain is therefore important to achieve the increase in bone mass and bone density to stabilize dental implants.

The study by Melsen & Lang (2001) support the theory that apposition of bone around dental implants is the biological response to a mechanical stress below a certain threshold. In their animal study, dental implants were inserted in Monkeys and continuous loading was applied after healing. Bone apposition was reported when the strain varied between 3,400 and 6,600 microstrains. When the strain reached 6,700 microstrains, the remodeling resulted in the net loss of bone.

A recent animal experimental study by Smet et al.(2008) studied whether controlled early loading enhances peri-implant bone mass and bone-to-implant contact. Low-frequency stimulation (3 Hz), with an optimum applied load that caused a strain of approximately 267 microstrains at 1.3mm from the implant, resulted in a significant positive effect on the difference in tibial bone mass in guinea-pigs. The authors concluded that force amplitude / strain at low frequency stimulation had an effect on the early control of mechanical stimulation of the peri-implant bone in the study model.

Mechanically, when occlusal loads are applied to dental implants, the stress will be transferred to the bone. When there are two materials with high different mechanical properties (i.e. stiffness), between dental implants and bone, the stress will be highest where the materials have first contact. The highest stress will therefore be expected in the most coronal portion of the supporting bone.

It is clinically difficult to quantify the magnitude or direction of naturally occurring occlusal forces, and even more to control or standardize these forces. Consequently, even though increased bone loss in areas of relatively high stress has been reported in some clinical studies, a causal relationship with overload has not been established (Isidor, 2008).

Ideal restorations can promote positive bone remodeling and minimize the healing time. However, it is a challenge to predict that the loaded implant will induce bone remodeling. Superstructure designs of dental implants, especially occlusal designs, may have an impact on bone strains around dental implants when occlusal loads are applied. As mentioned above, bone tissue reacts to strain (i.e., deformation), and if the strain in the bone surrounding dental implants is in the ‘mild overload’ range (1500–3000 microstrain), apposition of bone appears to be the biological response. However, it also depends on the properties of the bone tissue.

5. AIMS / HYPOTHESES OF THE INVESTIGATION

The study will investigate different occlusal designs in implant superstructure prostheses and associated loading changes.

Study - effects of loading

- This study aims to investigate strain peaks on bone simulated models to provide an understanding of the influence of various occlusal designs on implant-supported single crowns, for example, loading position and area of stress / strain distributions.
- To investigate the loading implications on implant-supported single crowns.
    - Hypothesis 1: Loading on the central area of the prosthesis along the long-axis of implants reduces strains on a simulated bone model surrounding dental implants.
- To investigate the effects of occlusal load on occlusal scheme design and dimensions in implant restorations.
    - Hypothesis 2: The appropriate occlusal form with reduced dimensions of the implant superstructure may reduce strains on a simulated bone model surrounding dental implants.

CHAPTER 2

MATERIALS AND METHODS

1. MATERIALS

1.1 THE BRÅNEMARK IMPLANT

Osseointegrated oral implants are available in different materials, shapes, diameters, lengths, platforms, surface properties and coatings. It has been estimated that dentists have a choice of more than 1,300 types of implants that vary in form, material, dimension, surface properties and interface geometry.

The Brånemark implant system is most widely used. The original two-stage implant protocol consists of several precision, interconnected components, with precision screw retention allowing retrievability of components. It is comprehensively documented.

1.1.1 The fixtures

The standard fixture is 3.75 mm in diameter and is available in several lengths: 7, 8.5, 10, 11.5, 13, 15 and 18 mm. In this study a 10 mm Brånemark system® Mk III fixture, regular platform Ø 3.75 mm diameter was used (figure II – 1).

Figure II – 1 A 10 mm Brånemark system® Mk III fixture, RP, Ø 3.75 mm

1.1.2 The abutment

The abutment used in this study was a titanium temporary abutment - Brånemark system® regular platform (figure II – 2) - which locked onto the implant fixture. An anti-rotational "hex" interlock between the base of the abutment and the top of the fixture provided retention. The temporary abutment was held in place with an abutment screw and the abutment was modified to a height of 5 mm.

Figure II – 2 Temporary abutment, Brånemark system®, RP

1.1.3 The abutment screwdriver

An abutment screwdriver was used to hand-tighten the titanium cylinder screw onto the temporary abutment. The manual screwdriver was available with unigrip and hex in different lengths to accommodate differing interocclusal distances. In this study a manual unigrip screwdriver, 14/29 mm, was used (figure II – 3).

Figure II – 3 A manual unigrip screwdriver, 14/29 mm

1.2 FIXATION OF THE IMPLANT

To simulate the in-vivo situation, the implants were embedded in moulds of acrylic resin; shaped to be similar to human jaw bone dimensions.

1.2.1 The acrylic resin mould

Moulds of acrylic resin were prepared to simulate the shape, size and structure of the jaw bone by using data from a computerised axial tomography (CT). Since human jaw bone varies individually, site-specific dimensions were selected for size and shape for the bone models. Four common implant sites from maxillary and mandibular arches, were

selected – anterior, canine, premolar, and molar regions – from CT scans with radiographic markers representing the position of the implant supported single crowns (figure II – 4 and figure II – 5). As the study focused on posterior mandibular segments, the shape of the bone model was therefore based on the mandibular premolar region. The bone model was constructed with a cross-section based on the size of the mandibular jaw from the CT scan (figure II – 6).

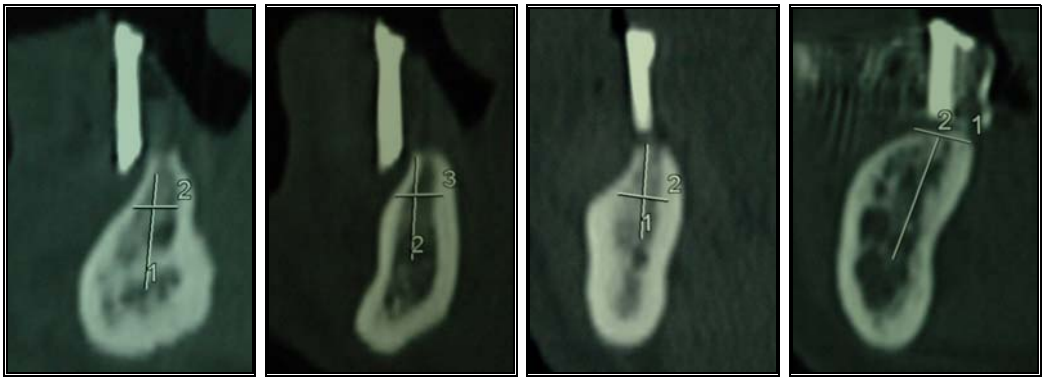

(a) (b) (c) (d)

Figure II – 4 Bone CT scan from (a) anterior mandible (b) canine mandible (c) premolar mandible (d) molar mandible

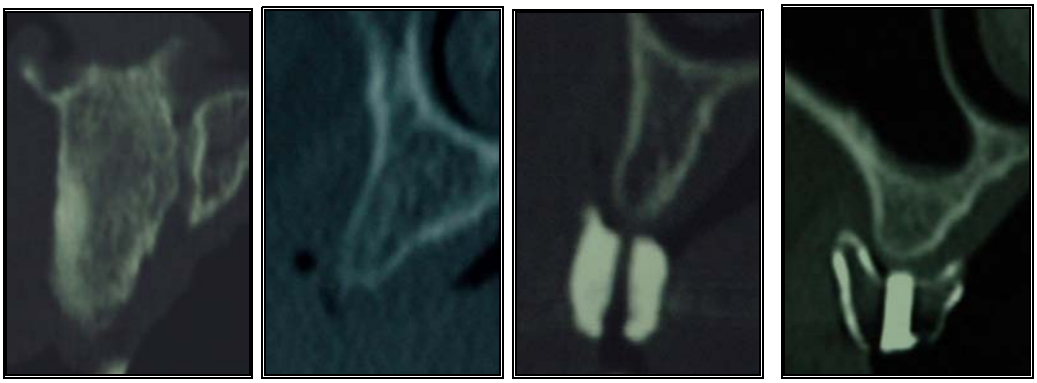

(a) (b) (c) (d)

Figure II – 5 Bone CT scan from (a) anterior maxllia (b) canine maxilla (c) premolar maxilla (d) molar maxilla

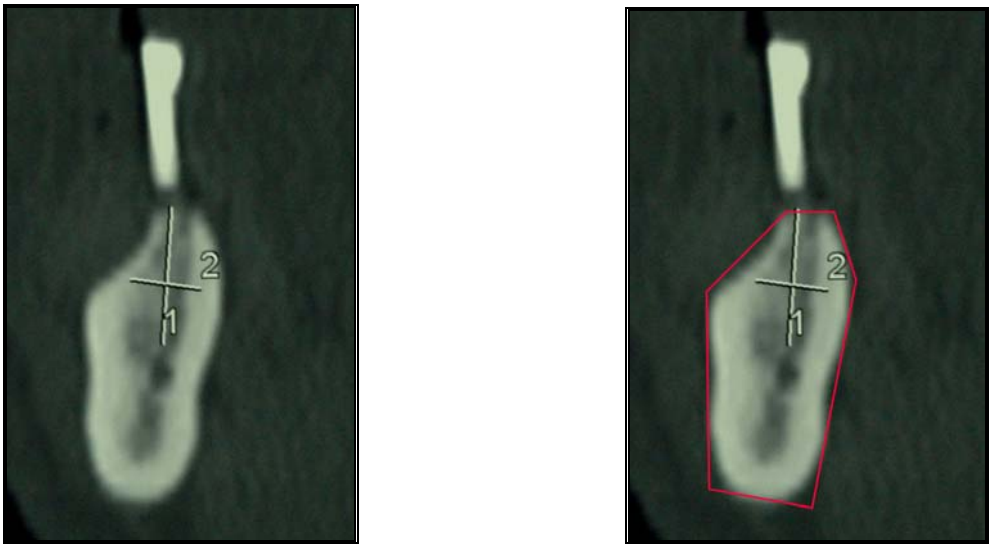

(a) (b)

Figure II – 6 (a) Bone CT scan from premolar mandible

(b) Simulated bone modeling in mandibular premolar region

Bone simulation models were made from clear heat-cured acrylic resin (Vertex™ Regular and Regular Crystal Clear, Vertex Dental B.V., Netherlands) following the manufacturer's instructions. To control the size and shape of the bone model, an invested plastic mould was constructed to receive a pour of pink wax, which was invested in a flask for the heat-processing of the acrylic resin models (figure II – 7).

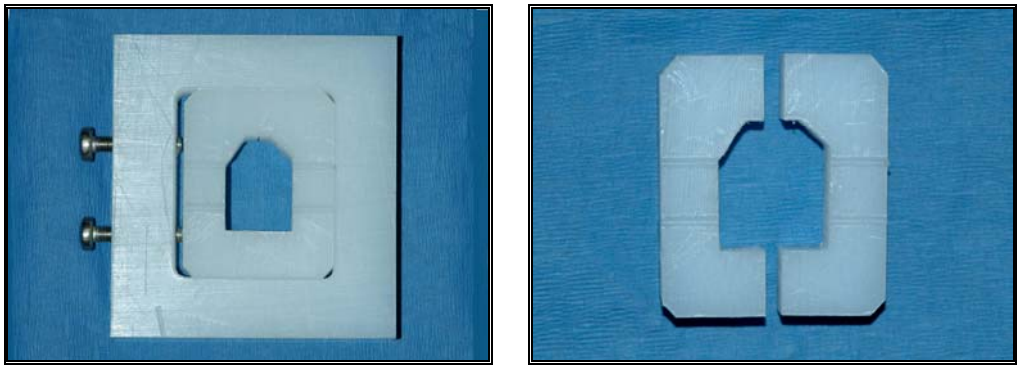

Figure II – 7 The plastic mould was constructed to control the size and shape of the simulated bone models.

1.2.2 Fixation in a composite resin simulated bone model

Regular platform 10-mm implant fixtures were placed in the simulated bone models, following the manufacturer's instructions.

1.3 SUPERSTRUCTURE

The superstructure prosthesis used in this study was of VITABLOCS Mark II®, which consisted of fine-particle feldspar ceramic (figure II – 8). VITABLOCS Mark II® were designed and constructed by using Cerec® 3D Sirona Dental Systems. Cerec® dental restorations use computer-assisted technologies, including 3D photography and CAD/CAM (computer-aided design/computer-aided manufacture).

.

In this study, the temporary abutment connected to the implant fixture was first photographed and stored as a three-dimensional digital model, and proprietary software was then used to approximate the restoration shape. The CEREC 3D software included three design techniques: dental database (with and without antagonist), correlation, and replication. Dental database design without antagonist was used to create the crown. The dental database method allowed the clinician to create a new restoration by selection from different databases of teeth stored in the software and had the flexibility to alter tooth morphology. The crown model was photographed perpendicular to the screen to measure cusp inclination and refined using 3D CAD software. The initial model was firstly modified with a milling machine to carve the restoration from the ceramic block with diamond burs under computer control. The Cerec® crown was verified for cusp inclination

and occlusal table dimension and was adjusted in the 3D CAD software. Once the design process for the tooth was completed and had resulted in the desirable tooth form, Cerec® crowns were milled for 10 specimens for each occlusal design.

The experimental occlusal design specimens were ceramic analogues of anatomic 30-degree and 10-degree teeth. The occlusal table dimensions were prepared as 3-mm or 6-mm occlusal crown widths (figure II – 9).

- Model one: 10 single tooth restorations – temporary abutments and ceramic crowns, with 30-degree cusp inclinations, and 6-mm occlusal table dimensions.
- Model two: 10 single tooth restorations – temporary abutments and ceramic crowns, with 30-degree cusp inclinations, and 3-mm occlusal table dimensions.
- Model three: 10 single tooth restorations – temporary abutments and ceramic crowns, with 10-degree cusp inclinations, and 6-mm occlusal table dimensions.
- Model four: 10 single tooth restorations – temporary abutments engaging and ceramic crowns, with 10-degree cusp inclinations, and 3-mm occlusal table dimensions.

Figure II – 8 VITABLOCS Mark II®, by Sirona Dental Company

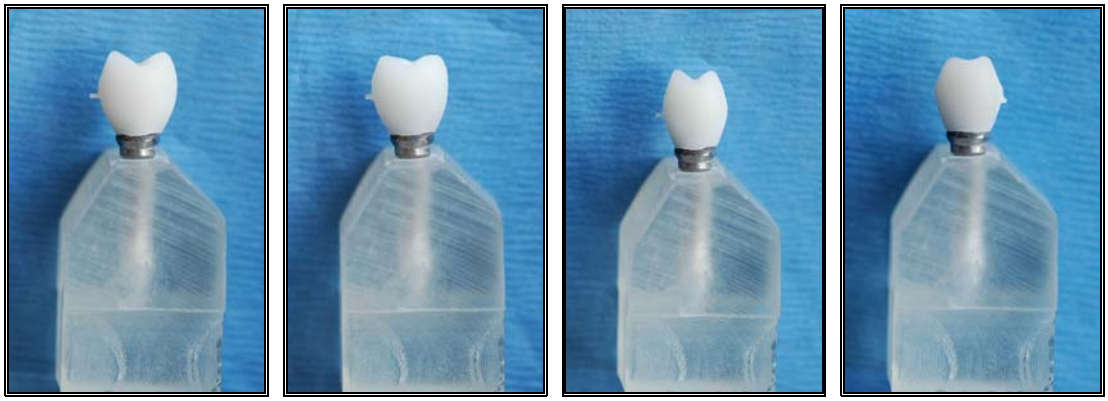

(a) (b) (c) (d)

Figure II – 9 Cerec® crowns in four different occlusal designs

(a) 30-degree cusp inclinations, and 6-mm occlusal table dimensions

(b) 10-degree cusp inclinations, and 6-mm occlusal table dimensions

(c) 30-degree cusp inclinations, and 3-mm occlusal table dimensions

(d) 10-degree cusp inclinations, and 3-mm occlusal table dimensions

1.4 THE MEASURING EQUIPMENT

1.4.1 Tri-axial miniature rosette strain gauges

Measurements of strain were made by experiments, and the important tool in experimental stress analysis was the electrical resistance strain gauge, which consisted of a wire grid or piece of metal foil bonded to the specimen. This device measured accurately the surface strain in the direction in which it was applied.

A cervical area of the simulated bone models were prepared with an abrasive and alcohol wipe before strain gauge placement. Three-element, 45-degree rectangular stacked rosette strain gauges of 120 ohm resistance (model WA-06-030 WR-120, Vishay Micro-Measurements Group Inc., Raleigh, North Carolina)(figure II – 10) were cemented on the cervical area of the bone simulation models with a thin film of methyl-2-cyanoacrylate resin (M-Bond 200 adhesive, Measurements Group Inc.).

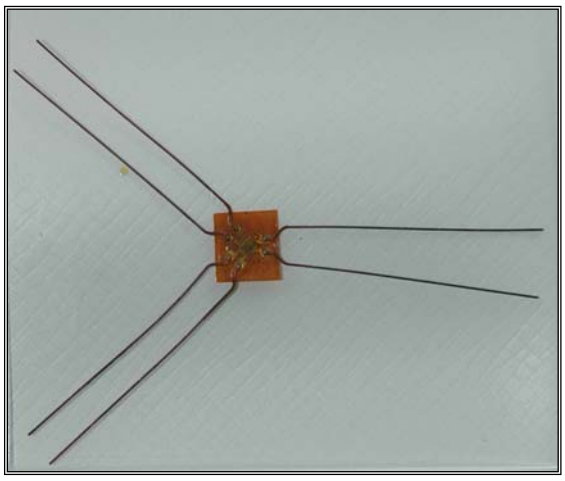

Figure II – 10 Strain gauges (model WA-06-030 WR-120, Vishay Micro-Measurements Group Inc., Raleigh, North Carolina)

The strain gauges were attached on a cervical area of buccal and lingual sides of the simulated bone models (figure II – 11). The area within the green line, which was referred to the buccal and lingual side of the bone simulated model, was divided into 9 parts. The middle part was selected to attach strain gauges (figure II – 12a and 12b). The location of strain gauge placement was based on the results of previous studies that reported a concentration of stress around the neck and apex of dental implants (Brunski, 2000 and Wang, 2002). Clinical studies showed that bone resorption occurred around the coronal zone of the implant (Isidor, 1997; Goodacre, 2003 and Misch, 2005). The strain gauges were placed on the possible closest area of the coronal zone of the bone simulated model to measure the strains developed when four different occlusal designs of superstructures were connected with implant fixtures.

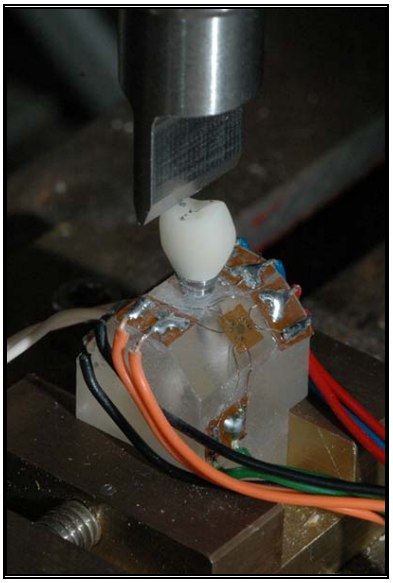

Figure II – 11 The strain gauges were attached on the cervical area of the simulated bone model.

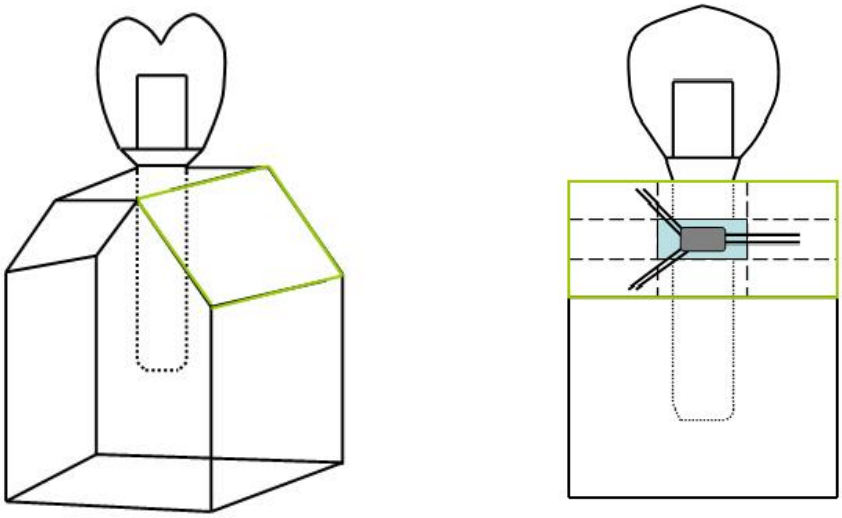

(a) (b)

Figure II – 12a and 12b Buccal and lingual sides of the bone simulated model within the green line were divided into 9 parts. The middle part was selected to attach strain gauges

It may not yet be defined in which directions present the greatest strains at the loading point. Therefore, Three-element, 45-degree rectangular stacked rosette strain gauges, with the gauge length and width of 0.76 mm for each section, were selected. The strain gauges were oriented in 3 directions (figure II – 13): strain gauge A and strain gauge B oriented at 90 degrees to each other and strain gauge C at 225 degrees to A. Strain gauge C was parallel to the horizontal direction of the buccal and lingual simulated bone model, and the other two strain gauges were aligned at 45 degrees to the horizontal.

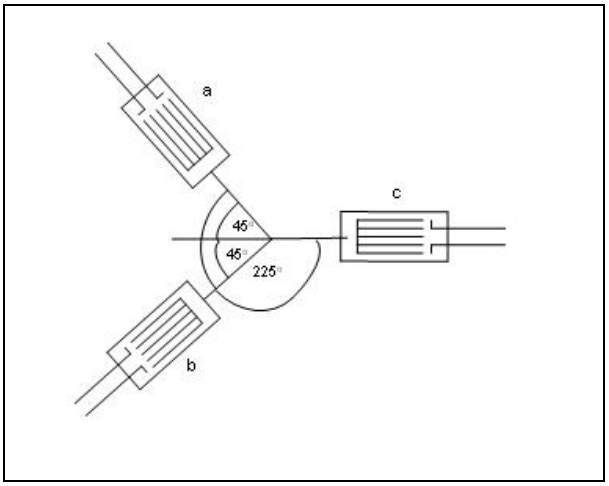

Figure II – 13 The 45-degree strain gauges were oriented in 3 directions: strain gauge A, strain gauge B 90 degrees to A and strain gauge C 225 degrees to A

The strain gauges were connected in series for measuring strain in 3 directions on buccal and lingual sides. Signals were collected with a National Instruments 16-Channel Universal Strain Gauge Input Module (NI SCXI-1520). The voltage supplied was 2.5V. Low-voltage excitation and adjustment were used to minimise temperature effects and voltage drift.

The circuit of the strain gauge is illustrated in figure II – 14. The change in strain-initiated resistance was very small, and a Wheatstone bridge was included in the circuit to convert the resistance change to a voltage for strain measurement. The strain gauge was connected to one side of the bridge and a fixed resistor was inserted into each of the other three sides. Output voltage, which was proportional to a change in resistance, i.e. a change in strain, was obtained. This output voltage was amplified for analog recording or digital indication of strain.

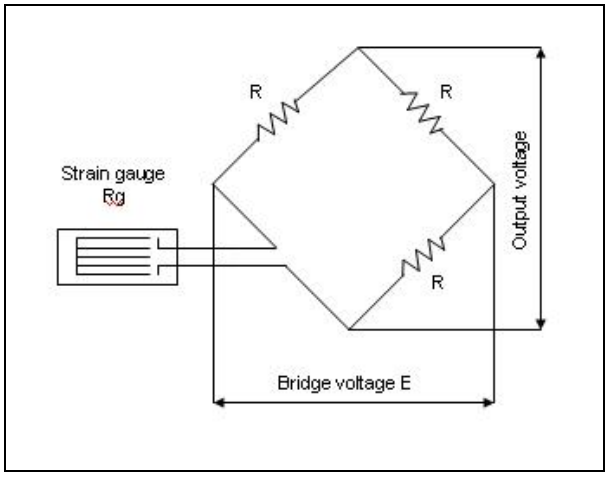

Figure II – 14 Simple circuit of strain gauge

1.4.2 Instron universal testing machine

Quantified axial forces were applied to the specimen by using an Instron 8874 universal testing system (Instron, MA, U.S.A.), which is a biaxial hydraulic system (figure II – 15). Specifications of the Instron 8874 are described in table II – 1.

Table II – 1 Specifications of Instron 8874 universal testing system (Instron, MA, U.S.A.)

Specifications	Instron 8874 universal testing system
Maximum Load Capacities	+/-10 kN to +/-25 kN
Power Supply	Requires additional 207 bar 3000 psi hydraulic supply
Standard Height	2359 mm (92.87 in)
Extra Height	2659 mm (104.69 in)
Overall Width	815 mm (32.1 in)
Overall Depth	483 mm (19.01 in)
Maximum Daylight: (Load Cell Actuator Mounted)	
Standard Height	733 mm (28.86 in)
Extra Height	1033 mm (40.67 in)
Maximum Daylight: (Load Cell Table Mounted)	
Standard Height	701 mm >(27.6 in)
Extra Height	1001 mm (39.4 in)
Column Spacing	455 mm (17.91 in)
Weight	300 kg (661 lb)

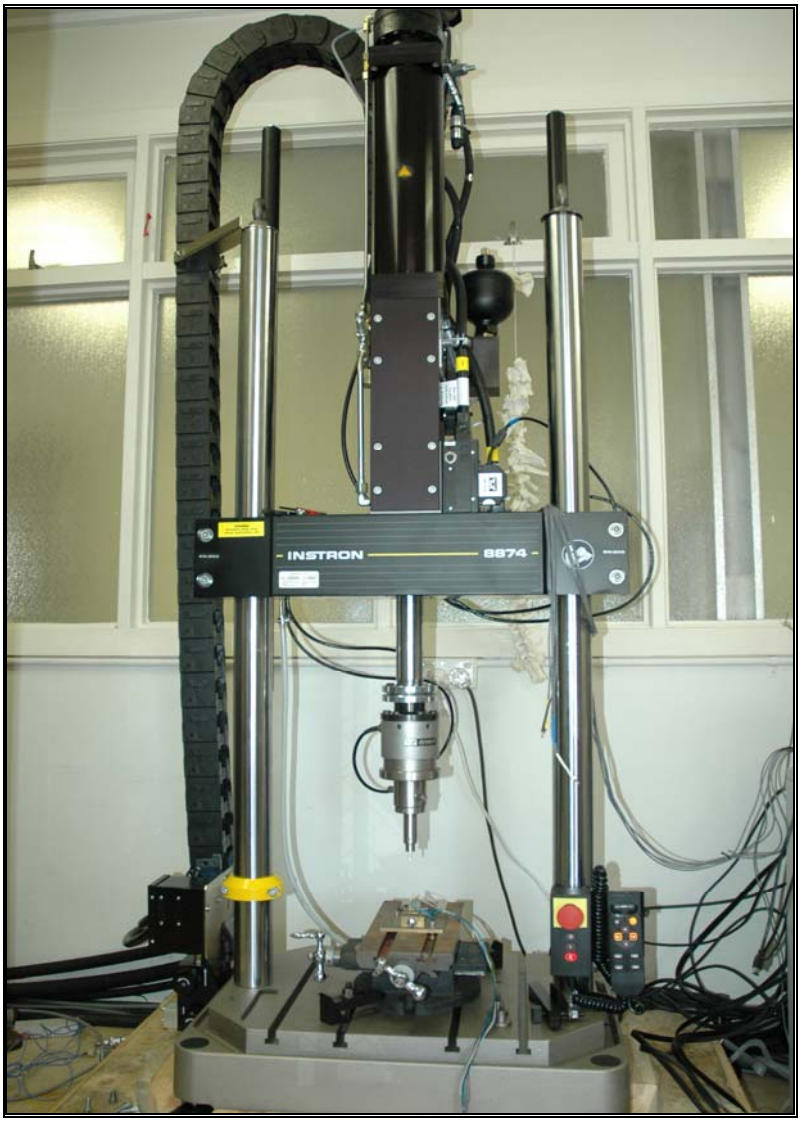

Figure II – 15 Instron 8874 universal testing system (Instron, MA, U.S.A.)

2. METHODS

2.1 STUDY DESIGN

This study was designed to determine the influence of different occlusal forms of the implant prostheses, and the associated loading changes on the implant system and simulated bone model. Four different occlusal crown designs were selected as representative of possible clinical occlusal forms. Each was tested under load to identify the effect of the changes in superstructure design on the simulated bone model.

Occlusal designs with respect to cusp height and crown width of implant-supported single crowns are possible. This study investigated a specific variations in occlusal design on an implant-supported single crown model.

2.1.1 Fabrication of test model and prostheses

A mould of acrylic resin was prepared to simulate the shape, size and structure of bone by using data from computerised axial tomography (CT). The bone model was constructed to mimic cross- sectional dimensions based on the size of the mandible as determined from the CT scans.

A regular platform 10-mm implant fixture was placed in the acrylic resin mould following the manufacturer's instructions.

The superstructure prosthesis: each implant supported a ceramic crowns as a single tooth restoration utilising a temporary abutment

engaging the regular platform and connected to the implant fixture. The experimental occlusal design specimens were constructed as a ceramic analog of anatomic 30-degree and 10-degree teeth. The occlusal tables were prepared with 3-mm or 6-mm occlusal table widths.

Passivity of the fit of the crowns was verified by one clinician.

Strain gauges were attached on the cervico-buccal and cervico-lingual area of the simulated bone model as previously described.

Diagram of implant-supported single crown with strain gauges attached on the buccal and lingual region of bone simulated model is seen in figure II – 16.

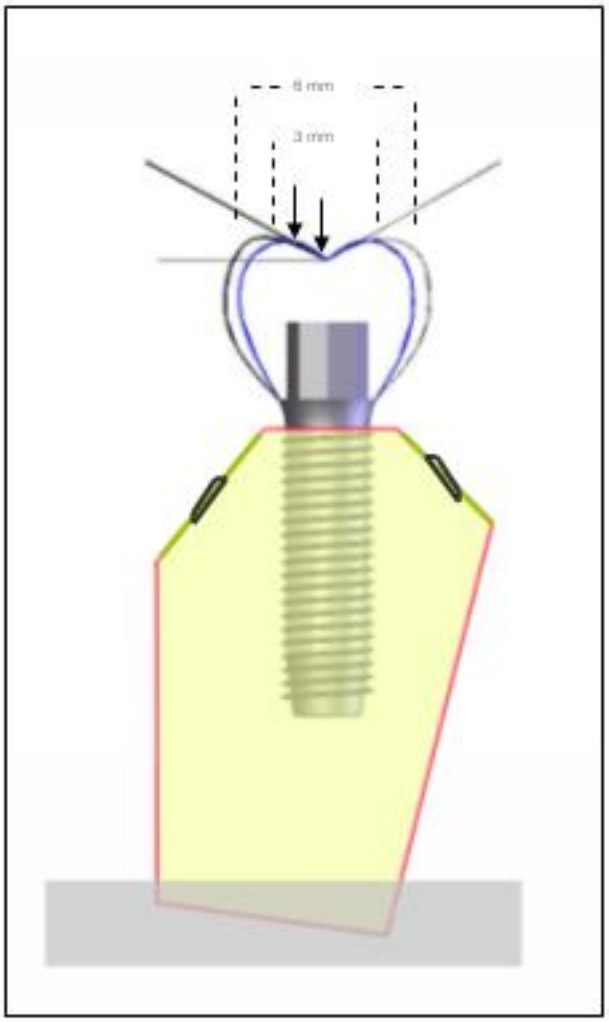

Figure II – 16 Experiment design for an implant-supported single crown with strain gauges attached on buccal and lingual area.

2.1.2 Determining the maximum force to be used

Determining the forces to be used in the study was based on the magnitude of forces possible in vivo.

Measurements of human bite forces generated intra-orally were obtained from a review of the literature. Estimated average biting forces of 125 N and maximum bite force of 400 N were reported

(Brånemark et al., 1977). Maximum vertical forces during the chewing cycle, with different textures of food, was found to be up to 121 N on implants in the posterior region, and 30 N for transverse forces (Richter, 1995). Mean maximum forces varied from 112.5 N to 450 N. Data from bite force studies in the healthy adult dentition were reported to be in the range of 469 N (canine) to 723 N (second molar), with lateral bite forces estimated at 20 N (Brunski, 2000).

In this study, axial forces of 50 N, 100 N, 150 N, 200 N and 250 N were applied to the specimens. Maximum axial forces were applied without causing to loosening or fracture of crowns.

2.1.3 Determining force and torque in 30- and 10-degree cusp inclinations and 3- and 6-mm occlusal table dimensions

Force and torque at the implant were calculated to determine the force and torque differences between each occlusal design before beginning the study.

The mathematical formulae (II – 1) were applied to calculate force and torque at the implant level. Axes of force were arranged at the angle θ as shown in figure II – 17.

$$F\cos\theta = Fx \qquad \text{(formulae II – 1)}$$

$$F\sin\theta = Fy$$

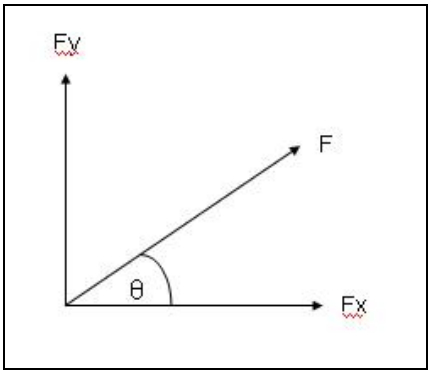

Figure II – 17 Axes of force were arranged at the angle θ

In this study, occlusal loading of 250 N (F) was applied axially, and the 2 mm buccally and in the middle of the occlusal table to define the loading positions. The height of the crown was set as 8 mm. The abutment height was 3 mm, and the distance from the fixture head to the third thread of the fixture was 3 mm (figure II – 18).

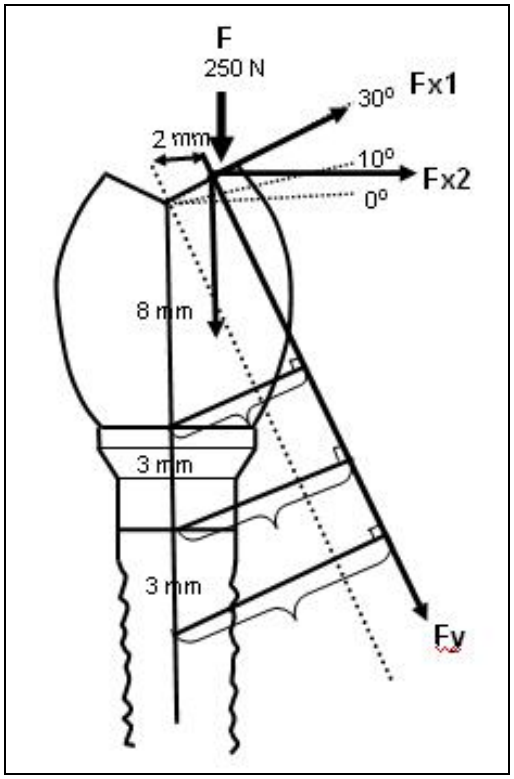

Figure II – 18 Diagram of dimensions of components of the implant-supported crown to calculate force and torque at the implant level.

Force

Forces in three axes were calculated for a 30-degree cusp inclination with 250 N axial force (F) applied (a) in the central fossa and (b) along the buccal incline 2 mm from the central fossa (figure II – 18).

Fx1	= Fcosθ	Fy	= Fsinθ
Fx1	= (250)(cos60)	Fy	= (250)(sin60)
Fx1	= 125 N	Fy	= 216.5 N

Fx2cosθ	= Fx1
(Fx2)(cos30)	= 125
Fx2	= 125/(cos30)
Fx2	= 144.34 N

Applying the mathematic formulae, the horizontal force (Fx1) on the superstructure with 30-degree cusp inclination was 144.34 N, and the non-axial force (Fy) with that cusp inclination was 216.5 N.

Forces in three axes were also calculated for a 10-degree cusp inclination with 250 N axial force (F) applied to the buccal inclined 2 mm from the central fossa (figure II – 18).

Fx1	= Fcosθ	Fy	= Fsinθ
Fx1	= (250)(cos80)	Fy	= (250)(sin80)
Fx1	= 43.41 N	Fy	= 246.2 N

$Fx2\cos\theta = Fx1$

$(Fx2)(\cos 10) = 43.41$

$Fx2 = 43.41/(\cos 10)$

$Fx2 = 44.08\ N$

The horizontal force (Fx1) on the crown with a 10-degree cusp inclination was 44.08 N, and non-axial force (Fy) with that cusp inclination was 246.2 N. Horizontal force of 10-degree cusp inclination was therefore less than that of 30-degree cusp inclination.

Magnitude of torque

Torque (moment) is the force multiplied by the perpendicular distance from the line of force. Therefore, implant distance multiplied by force (Fy) was calculated to establish the torque (Figure II – 18)

0-degree cusp inclination

Torque = Fy x D

T = (250)(2)

T = 500 N

10-degree cusp inclination

$\text{Sin } 10^0$ = D/(8+3+3)

D = $(14)(\text{Sin } 10^0)$

D = 2.43

Implant distance = D + 2

= 2.43 + 2

= 4.43

	Torque	=	F x D
	T	=	(246.2)(4.43)
	T	=	1091 N-mm
30-degree cusp inclination	Sin 30^0	=	D/(8+3+3)
	D	=	(14)(Sin 30^0)
	D	=	7
	Implant distance	=	D + 2
		=	7 + 2
		=	9
	Torque	=	F x D
	T	=	(216.5)(9)
	T	=	1948.5 N-mm

Torque on the crown with 10-degree cusp inclination was 1091 N-mm, whereas that of the crown with a 30-degree cusp inclination was 1948.5 N-mm.

There was no difference between force and torque with 3- and 6-mm occlusal table dimensions. However, force and torque were not represented as surface strain on the simulated bone model because surface strain would depend on the geometry of the model, material properties and location of strain measurement. Force and torque were calculated on the hypothesis that there would be a possible difference between each occlusal design. Experimental method was

necessarily set up for determining the surface strain of each occlusal design.

2.2 STUDY METHODS

2.2.1 Test load levels and positions

Static loads from 50 N to 250 N were applied for 15 seconds and recorded. The applied forces were loaded on two loading sites (figure II – 19). The central area and 2 mm buccally were selected at the middle of the occlusal table for each specimen, to define the loading position and direction of loading.

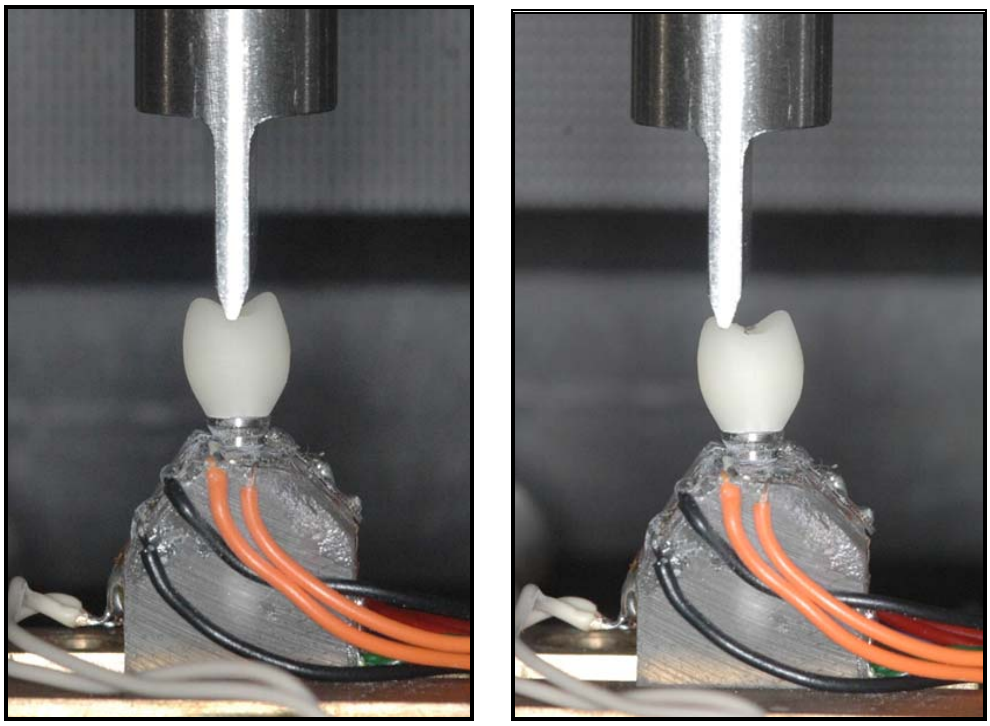

Figure II – 19 The applied forces were loaded on two loading sites: the central fossa area and 2 mm buccally.

2.2.2 Experimental design and test procedure

Static tests were performed using a computer-controlled precision universal testing machine (INSTRON 8874 biaxial hydraulic testing system) in the load control mode.

Each specimen was appropriately adjusted on the platform, to ensure that the loading unit made contact at the desired loading position (Figure II – 20). The crosshead distance was controlled by the handle; a ruler was used to measure the distance from the central area to 2 mm buccally (Figure II – 21).

Static tests were performed on the universal testing machine at room temperature, and the crosshead speed was set at 0.05 mm/min to eliminate impacts.

A series of five axial forces were applied ten times to each of the occlusal-design specimens. This procedure was repeated for 30-degree cusp inclination and 6-mm bucco-lingual occlusal width, 30-degree cusp inclination and 3-mm bucco-lingual occlusal table width, 10-degree cusp inclination and 6-mm bucco-lingual occlusal table width and 10-degree cusp inclination and 3-mm bucco-lingual occlusal table width.

After each series of axial force applications, the instrument was balanced. A computer was connected with the bridge amplifier to

record output signals of strains and baseline deflections from the strain gauges (Figure II – 22). All test results, including the test condition, specimens, and load-deflection data were automatically recorded and stored by a data acquisition system installed to provide a database for carrying out statistical calculations.

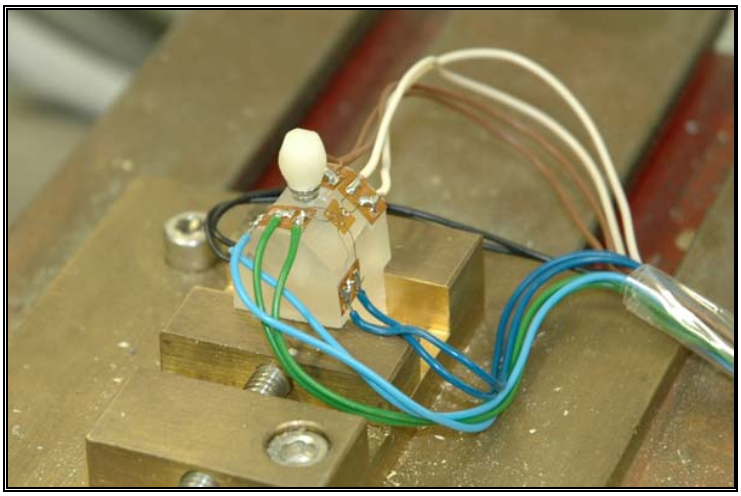

Figure II – 20 Each specimen was appropriately adjusted on the platform

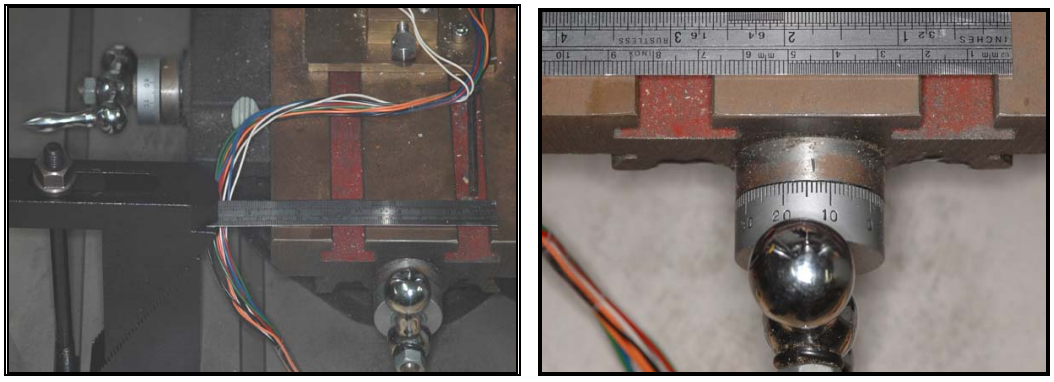

Figure II – 21 The crosshead distance was controlled by the handle; a ruler was used to measure the distance from the central area to 2 mm buccally.

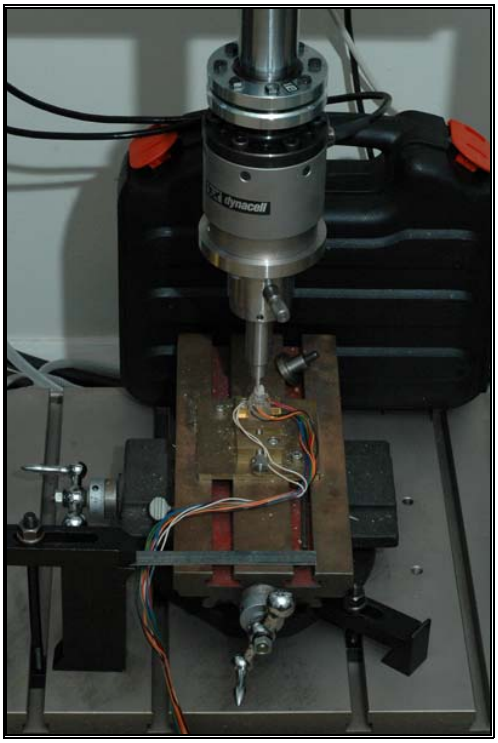

Figure II – 22 Study models were tested using a universal testing machine. A computer was connected with the bridge amplifier to record output signals of the simulated bone strains and baseline deflections from the strain gauges.

2.3 DATA ANALYSIS

Data were collected for strain values. Strain values from each strain gauge were used to determine the maximum principal strain, which represented the largest baseline deflection at the buccal and lingual of the cervical areas of the simulated bone model.

Defining of strain

When a force is applied, it will tend to change the shape and size of the specimen. These changes are referred to as deformation. Strain at the point of contact is defined by specifying normal strain and shear strain.

Normal strain is a measure of a deformation by changes in length of line segments. The ratio of the elongation to the original length when a material receives a tensile force (P) is called a tensile strain and is expressed by the formula II – 2 and figure II – 23:

$$\varepsilon = \frac{\Delta L}{L} \qquad \text{(II – 2)}$$

ε = strain

L = original length

ΔL = elongation

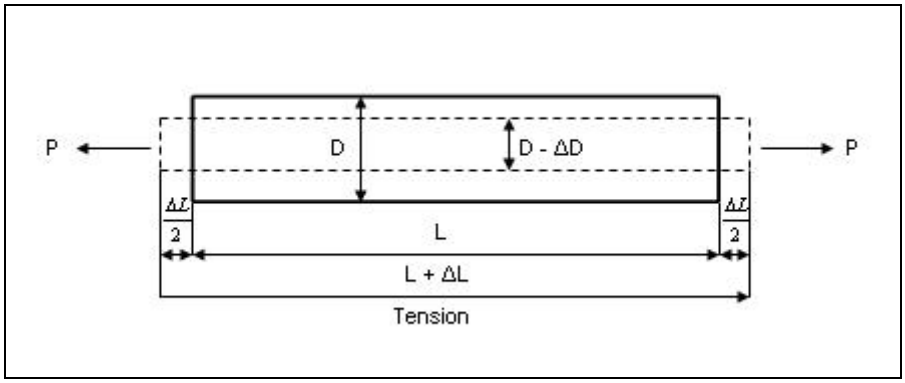

Figure II – 23 The ratio of the elongation to the original length when a material receives a tensile force (P)

Therefore, normal strain is a dimensionless quantity, since it is a ratio of two lengths. In most engineering applications strain will be very small, so measurements of strain are in micrometers per meter (μm/m), where 1 μm = 10^{-6} m.

Shear strain is a measure of the change in the angles which occur between two small line segments that are originally perpendicular to one another. This angle is denoted by γ and is measured in radians.

As a result, the deformation of the body may be defined by using the above definitions of normal and shear strain. To do so, the rectangular volume element of the material located at the point is considered, and the undeformed dimensions Δx, Δy, Δz are originally parallel to the x, y and z axes (figure II – 24). The strains completely describe the deformation of a rectangular volume element of material located at the point. The state of strain at the point is characterized by six strain components: three normal strains ε_x, ε_y, ε_z and three shear strain γ_{xy}, γ_{yz}, γ_{xz}. These six components

tend to deform each face of an element of the material, and the normal and shear strain components will vary according to the orientation of the element.

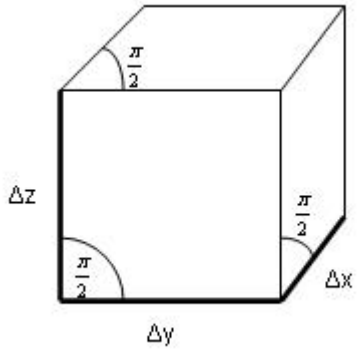

Figure II – 24 The rectangular volume element of the material located at the point of load contact is indicated, and the undeformed dimensions, Δx, Δy, Δz, are originally parallel to the x, y and z axes.

Strain components at a point are often determined by using strain gauges, which measure these components in specified directions. To do so, plane strain is used to specify the strain elements, which is subjected to two components of normal strain, ε_x, ε_y, and one component of shear strain, γ_{xy}. The deformations of an element caused by each of these strains are shown in figure II – 25.

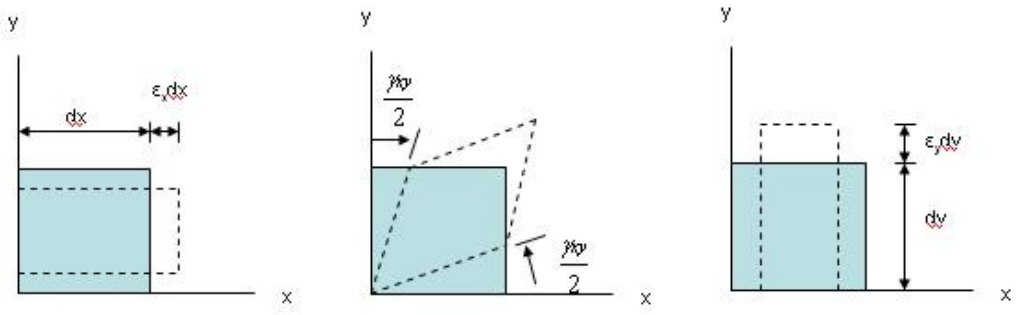

(a) (b) (c)

Figure II – 25

(a) and (c) The deformations of an element caused by two components of normal strain, ε_x and ε_y respectively.

(b) The deformations of an element caused by one component of shear strain (γ_{xy}).

In this study, three electrical-resistance strain gauges were used to specify the state of strain at the point only in the plane of the gauges. The axes of the three strain gauges were arranged at the angles Θ_a, Θ_b, Θ_c as shown in figure II – 26.

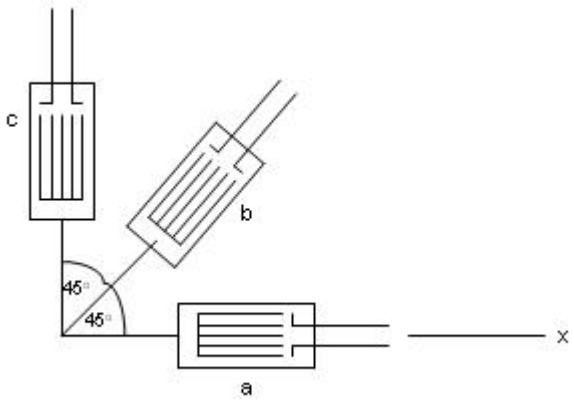

Figure II – 26 The axes of the three strain gauges were arranged at the angles Θ_a, Θ_b, Θ_c.

When the readings ε_a, $\varepsilon_{b,}$ ε_c were taken from the raw data; the strain components ε_x, $\varepsilon_{y,}$ γ_{xy} were determined at the point by applying the strain-transformation equation, for each gauge (equation II -1)(Hibbeler, 2003).

$$\varepsilon_a = \varepsilon_x \cos^2 \Theta_a + \varepsilon_y \sin^2 \Theta_a + \gamma_{xy} \sin \Theta_a \cos \Theta_a$$
$$\varepsilon_b = \varepsilon_x \cos^2 \Theta_b + \varepsilon_y \sin^2 \Theta_b + \gamma_{xy} \sin \Theta_b \cos \Theta_b \qquad \text{(II -1)}$$
$$\varepsilon_c = \varepsilon_x \cos^2 \Theta_c + \varepsilon_y \sin^2 \Theta_c + \gamma_{xy} \sin \Theta_c \cos \Theta_c$$

In this study, strain rosettes were arranged in 45^o or rectangular patterns shown in figure II – 26. Therefore, $\Theta_a = 0^o$, $\Theta_b = 45^0$, $\Theta_c = 90^0$, were replaced in equation II – 1 as demonstrated below, so that gives equation II – 2a-c (Hibbeler, 2003).

$$\varepsilon_a = \varepsilon_x \cos^2 \Theta_a + \varepsilon_y \sin^2 \Theta_a + \gamma_{xy} \sin \Theta_a \cos \Theta_a$$
$$\varepsilon_a = \varepsilon_x \cos^2 0^o + \varepsilon_y \sin^2 0^o + \gamma_{xy} \sin 0^o \cos 0^o$$
$$\varepsilon_a = \varepsilon_x(1) + \varepsilon_y(0) + \gamma_{xy}(0)(1)$$
$$\varepsilon_x = \varepsilon_a \qquad \text{(II – 2a)}$$

$$\varepsilon_c = \varepsilon_x \cos^2 \Theta_c + \varepsilon_y \sin^2 \Theta_c + \gamma_{xy} \sin \Theta_c \cos \Theta_c$$
$$\varepsilon_c = \varepsilon_x \cos^2 60^0 + \varepsilon_y \sin^2 60^0 + \gamma_{xy} \sin 60^0 \cos 60^0$$
$$\varepsilon_c = \varepsilon_x(0) + \varepsilon_y(1) + \gamma_{xy}(0)(1)$$
$$\varepsilon_y = \varepsilon_c \qquad \text{(II – 2b)}$$

$$\varepsilon_b = \varepsilon_x \cos^2 \Theta_b + \varepsilon_y \sin^2 \Theta_b + \gamma_{xy} \sin \Theta_b \cos \Theta_b$$

$$\varepsilon_b = \varepsilon_a(\frac{1}{2}) + \varepsilon_c (\frac{1}{2}) + \gamma_{xy}(\frac{1}{2})$$

$$\gamma_{xy} = 2\ \varepsilon_b - (\varepsilon_a + \varepsilon_c) \qquad (\text{II} - 2c)$$

To determine the maximum and minimum in-plane normal strain, this particular set of values are called the principle strain, and the corresponding planes on which they act are called the principle planes of strain. In this study, maximum principle strains, which is the element's deformation represented by normal strain with no shear strain, were determined.

Once ε_x, ε_y, γ_{xy} were determined from equation II – 2a-c, the maximum and minimum of the principal strains (ε_1 and ε_2) were determined from equation II – 3 (Hibbeler, 2003).

$$\varepsilon_{1,2} = \frac{\varepsilon_x + \varepsilon_y}{2} \pm \sqrt{\left(\frac{\varepsilon_x - \varepsilon_y}{2}\right)^2 + \left(\frac{\gamma_{xy}}{2}\right)^2} \qquad (\text{II} - 3)$$

In this study, only maximum principal strain (ε_1) was calculated for each occlusal design specimen.

The study variables: maximum principal strains for model one (30-degree cusp inclination with 6-mm occlusal table dimension), model two (30-degree cusp inclination with 3-mm occlusal table dimension), model three (10-degree cusp inclination with 6-mm occlusal table dimension), and model four (10-degree cusp inclination with 3-mm occlusal table dimension) were compared and analysed using the Univariate Analysis of Variance (ANOVA)

with Bonferroni as the post-hoc adjustment for multiple comparisons. A significance level of 5% ($P < 0.05$) was applied throughout the analysis. The statistical software SPSS (version 12) was used by defining the maximum principal strain as a dependent variable; and cusp inclination, occlusal table dimension, position, side and force levels as fixed factors.

CHAPTER 3

RESULTS

1. DATA ANALYSIS

The strain on the cervico-buccal and cervico-lingual area of the simulated bone model in figure II – 12a-b and II – 16 were measured using the strain gauges previously described.

The strain values (microstrains) were collected in six channels, three channels from the cervico-buccal area of the simulated bone model and the other three channels from the cervico-lingual area of the simulated bone model. A total of approximately six thousand strain values from the raw data in each test were plotted. An example of the line plot of raw data in the first test, measuring the strains from 30-degree cusp inclination with 6-mm occlusal table dimension with applied load at 2 mm, is shown in figure III – 1. The optimal ranges of raw data were then selected as the representative data for each series of applied forces from 50 N to 250 N. For example, in figure III – 1, raw data values ranged from 1,000 – 1,500 represented the strains (microstrains) with an applied force of 50 N; raw data values ranged from 2,000 – 2,600, 3,000 – 3,600, 4,000 – 4,600, 5,000 – 5,600 represented the strains (microstrains) with applied forces of 100 N, 150 N, 200 N and 250 N, respectively.

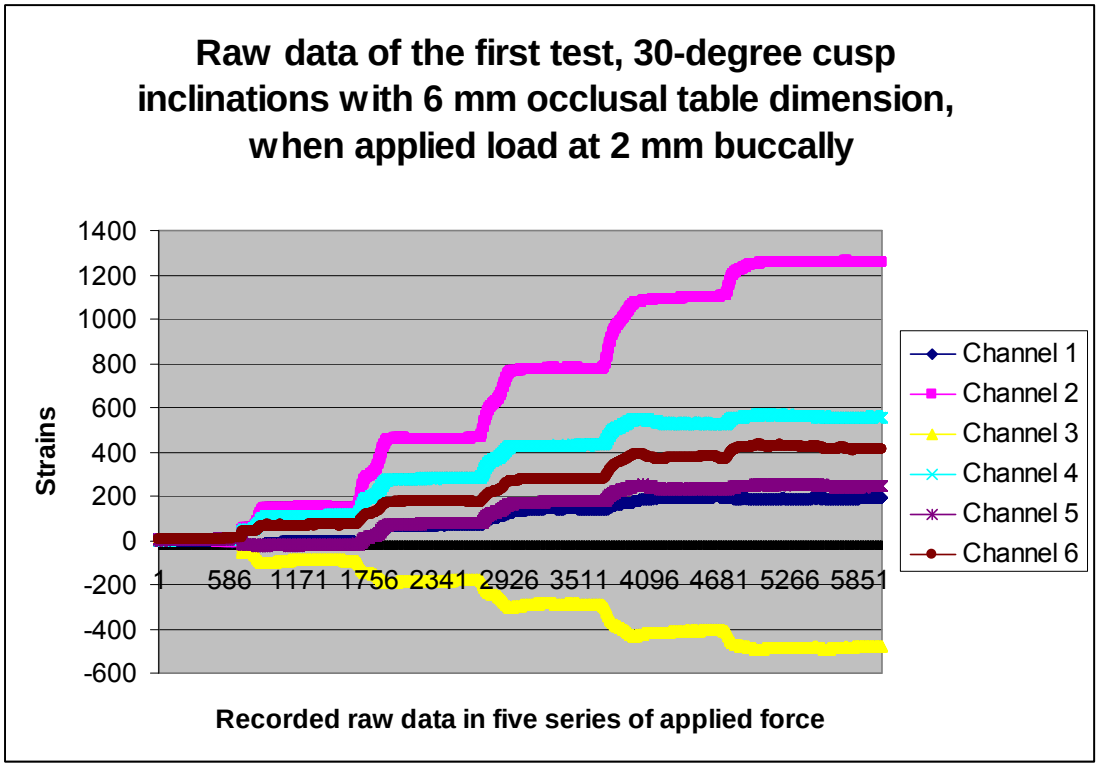

Figure III – 1 Line graph from raw data, measuring the strains (microstrains) from 30-degree cusp inclination with 6-mm occlusal table dimension with an applied load at 2 mm buccally.

Due to the series of applied forces, the readings from the gauges gave ε_a, ε_b and ε_c as indicated by channel 1, 2 and 3 for the strains at the contact point on the cervico-buccal area of the simulated bone model, and in channel 4, 5 and 6 for the strains at the contact point on the cervico-lingual area of the simulated bone model. The strain components ε_x, ε_y, γ_{xy} from each test were then determined by applying the strain-transformation equation for each gauge, as described in equation II -1 and II – 2a-c (Hibbeler, 2003), and then the maximum of the principal strains (ε_1) were calculated from equation II – 3 (Hibbeler, 2003).

Maximum principal strains (ε_1) were calculated in the unit of microstrains for each occlusal design for ten tests. Then all data were plotted in boxplots to detect systematic and skewed distributions of data.

Box and whisker plots were graphs of a five number summary. Box and whisker plots were appropriate for comparing similar distributions visually. The centre, spread and overall range were readily apparent. In box and whisker plots:

- the ends of the box were the upper and lower quartiles, so the box spaned the interquartile range;
- the median is marked by a vertical line inside the box; and
- the whiskers are the two lines outside the box that extend to the highest and lowest recordings.

This details are presented in figure III – 2 below:

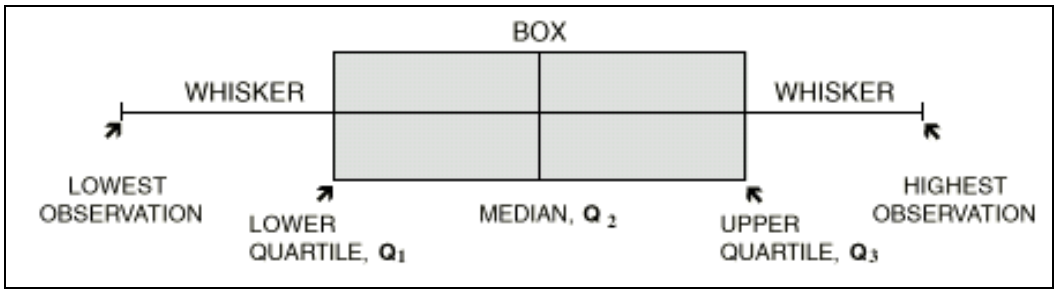

Figure III – 2 Box and whisker plot used to detect systematical and skewed data distribution.

In this study, the outlying scores presented in some data of each occlusal design were removed as the data were skewed.

The experimental variables - maximum principal strains for model one (30-degree cusp inclination with 6-mm occlusal table dimension), model two (30-degree cusp inclination with 3-mm occlusal table dimension), model three (10-degree cusp inclination with 6-mm occlusal table dimension), and model four (10-degree cusp inclination with 3-mm occlusal table dimension) were compared and analysed using the Univariate Analysis of Variance (ANOVA) with Bonferroni as the post-hoc adjustment for multiple comparisons. A significance level of 5% ($P < 0.05$) was applied throughout the analysis.

2. RESULTS

The experimental data were gathered in maximum principal strains (microstrains), which represented the largest baseline deflection registered by the strain gauges on the simulated bone model. The tables of raw data are listed in the appendices.

2.1 EFFECT OF CUSP INCLINATION AND OCCLUSAL TABLE DIMENSION

Experimental data and statistical evaluation are presented in tables III – 1 to III – 4 and figures III – 3 to III – 6, as mean maximum principal strains (microstrains) ± standard deviation (SD) for different loading conditions and occlusal designs.

2.1.1 *Experimental data and analyses for maximum principal strains (microstrains) for four different occlusal designs with applied loading at 2 mm on the buccal inclined plane and strain gauges attached on buccal side.*

Table III – 1 Microstrains of four different occlusal design under loading at 2 mm buccal inclined plane with the strain gauges attached on buccal side.

Occlusal designs	Cusp inclination (degree)	Occlusal table dimension	Forces (N)	Mean maximum principal strains (microstrains)	SD
Model 1	30	6mm	50	163.43	16.60
			100	472.98	21.30
			150	774.76	44.11
			200	1087.76	44.34
			250	1258.99	14.54
			Total	811.52	395.19
Model 2	30	3mm	50	42.57	5.93
			100	93.10	5.69
			150	146.44	9.90
			200	192.66	8.82
			250	231.85	6.10
			Total	141.32	68.79
Model 3	10	6mm	50	48.15	3.28
			100	104.70	3.31
			150	167.28	5.73
			200	240.84	5.84
			250	316.82	13.71
			Total	177.40	99.25
Model 4	10	3mm	50	5.10	0.83
			100	32.98	2.37
			150	68.85	2.12
			200	112.58	3.50
			250	156.98	4.47
			Total	75.30	55.31

F: 4032.91

Occlusal design: model 1 and model 2 (P:0.000); model 1 and model 3 (P:0.000); model 1 and model 4 (P:0.000); model 2 and model 3 (P:0.000); model 2 and model 4 (P:0.000); model 3 and model 4 (P:0.000) (post hoc test).

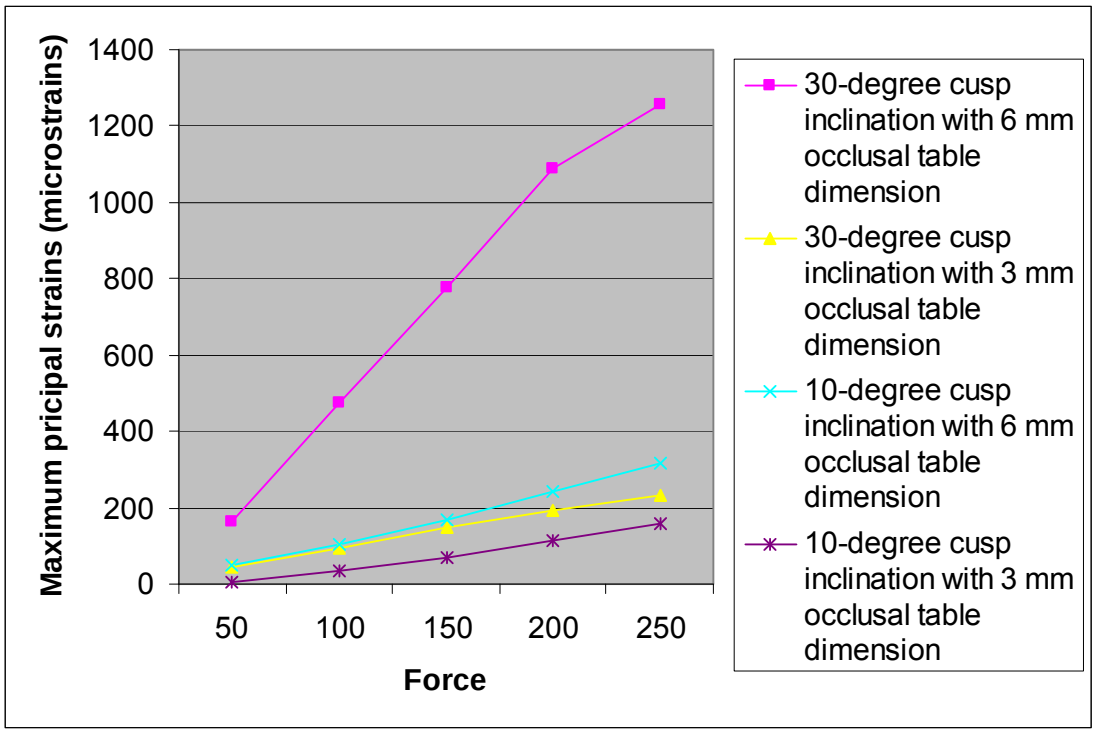

Figure III – 3 Microstrains of four different occlusal design specimens under loading applied at 2 mm on the buccal inclined plane with the strain gauges attached on buccal side.

The following observations may be made from table III – 1 and figure III – 3:

a) Maximum principal strains (microstrains) increased significantly when applied series of axial loading increased from 50 N to 250 N.

b) Highest maximum principal strain (microstrains), 811.52, was seen in the model one - 30-degree cusp inclination with 6-mm occlusal table dimension.

c) Model three - 10-degree cusp inclination with 6- mm occlusal table dimension - had slightly higher maximum principal strain (microstrains) on the simulated bone model, compared with the model two - 30-degree cusp inclination with 3-mm occlusal table dimension, and the lowest was presented in model four - 10-degree cusp inclination with 3-mm occlusal

table dimension. The maximum principal strains (microstrains) were defined as a dependent variable, while occlusal designs were defined as a fixed factor.

d) The Univariate Analysis of Variance (ANOVA) with post hoc test comparing the maximum principal strains (microstrains) for four different occlusal design specimens indicated a significant difference of the maximum principal strains (microstrains) between model one, two, three, and four, when an applied axial loading at 2 mm buccal on the inclined plane with strain gauges attached on the buccal side of the bone simulated model ($p = 0.000$).

2.1.2 *Experimental data and analyses for maximum principal strains (microstrains) for four different occlusal design specimens with applied loading at 2 mm on the buccal inclined plane and strain gauges attached on lingual side.*

Table III – 2 Microstrains of four different occlusal design specimens under loading at 2 mm on the buccal inclined plane with the strain gauges attached on lingual side.

Occlusal designs	Cusp inclination	Occlusal table dimension	Forces	Mean maximum principal strains (microstrains)	SD
Model 1	30	6mm	50	191.12	24.11
			100	361.38	33.20
			150	501.37	37.19
			200	653.46	31.60
			250	725.94	34.96
			Total	503.71	193.33
Model 2	30	3mm	50	51.01	7.88
			100	94.11	5.09
			150	135.24	7.90
			200	174.44	7.58
			250	209.37	9.21
			Total	133.62	57.55
Model 3	10	6mm	50	38.04	7.45
			100	86.29	18.19
			150	135.41	18.05
			200	188.34	34.87
			250	220.59	29.18
			Total	138.30	70.86
Model 4	10	3mm	50	47.49	8.87
			100	80.55	9.59
			150	110.76	10.68
			200	144.85	14.96
			250	200.09	29.53
			Total	114.30	54.33

F: 677.971

Occlusal design: model 1 and model 2 (P:0.000), model 1 and model 3 (P:0.000), model 1 and model 4 (P:0.000), model 2 and model 3 (P:1.000), model 2 and model 4 (P:0.001), model 3 and model 4 (P:0.000) (post hoc test)

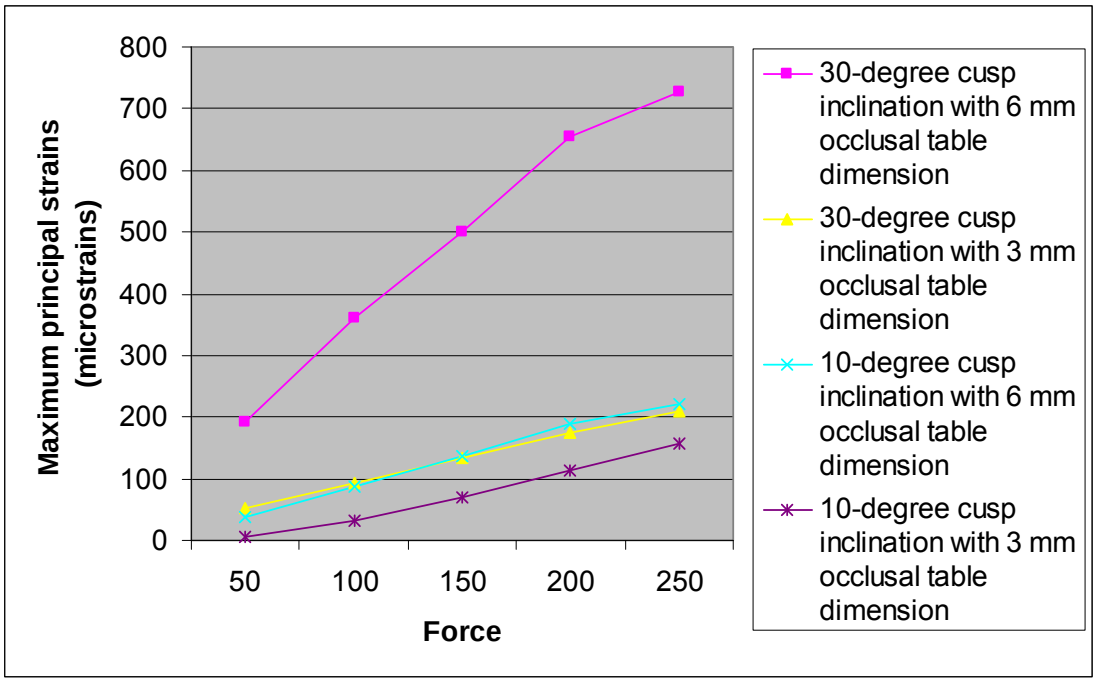

Figure III – 4 Microstrains of four different occlusal design specimens under loading at 2 mm on the buccal inclined plane with the strain gauges attached on the lingual side

The following observations may be made from table III – 2 and figure III – 4:

a) Maximum principal strains (microstrains) were increased significantly with the applied series of axial loads from 50 N to 250 N.

b) The highest maximum principal strain (microstrains) of 503.71 was seen in model one - 30-degree cusp inclination with 6-mm occlusal table dimension, whereas the lowest of 114.30 was seen in the model four - 10-degree cusp inclination with 3-mm occlusal table dimension. The maximum principal strains (microstrains) were defined as a dependent variable, while occlusal designs were defined as a fixed factor.

c) The Univariate Analysis of Variance (ANOVA) with post hoc test comparing the maximum principal strains (microstrains) for four different occlusal design specimens indicated significant differences of the maximum principal strains (microstrains) between the model one, two, three, and four, with an applied axial loading at 2 mm buccal on the inclined plane and strain gauges attached on the buccal side of the bone simulated model ($p = 0.000 – 0.001$). However, no statistical differences ($p = 1.000$) were found between the maximum principal strains (microstrains) of the model two - 30-degree cusp inclination with 3-mm occlusal table dimension and model three - 10-degree cusp inclination with 6-mm occlusal table dimension.

2.1.3 *Experimental data and analyses for maximum principal strains (microstrains) for four different occlusal design specimens when applied loading at central fossa and strain gauges attached on buccal side.*

Table III – 3 Microstrains of four different occlusal design specimens under loading at central fossa with the strain gauges attached on buccal side

Occlusal designs	Cusp inclination	Occlusal table dimension	Forces	Mean maximum principal strains (microstrains)	SD
Model 1	30	6mm	50	22.37	5.80
			100	68.94	11.35
			150	125.42	18.64
			200	178.12	19.07
			250	221.44	21.21
			Total	128.71	72.96
Model 2	30	3mm	50	14.58	11.14
			100	22.72	13.05
			150	31.12	22.34
			200	44.71	28.29
			250	67.73	29.49
			Total	40.37	29.79
Model 3	10	6mm	50	41.80	24.86
			100	44.31	8.76
			150	73.17	13.46
			200	109.85	16.78
			250	155.34	18.20
			Total	92.18	46.34
Model 4	10	3mm	50	18.11	5.15
			100	42.98	5.23
			150	71.52	4.38
			200	105.10	11.82
			250	141.39	14.87
			Total	75.82	45.27

F: 94.96

Occlusal design: model 1 and model 2 (P:0.000), model 1 and model 3 (P:0.000), model 1 and model 4 (P:0.000), model 2 and model 3 (P:0.000), model 2 and model 4 (P:0.000), model 3 and model 4 (P:0.001) (post hoc test)

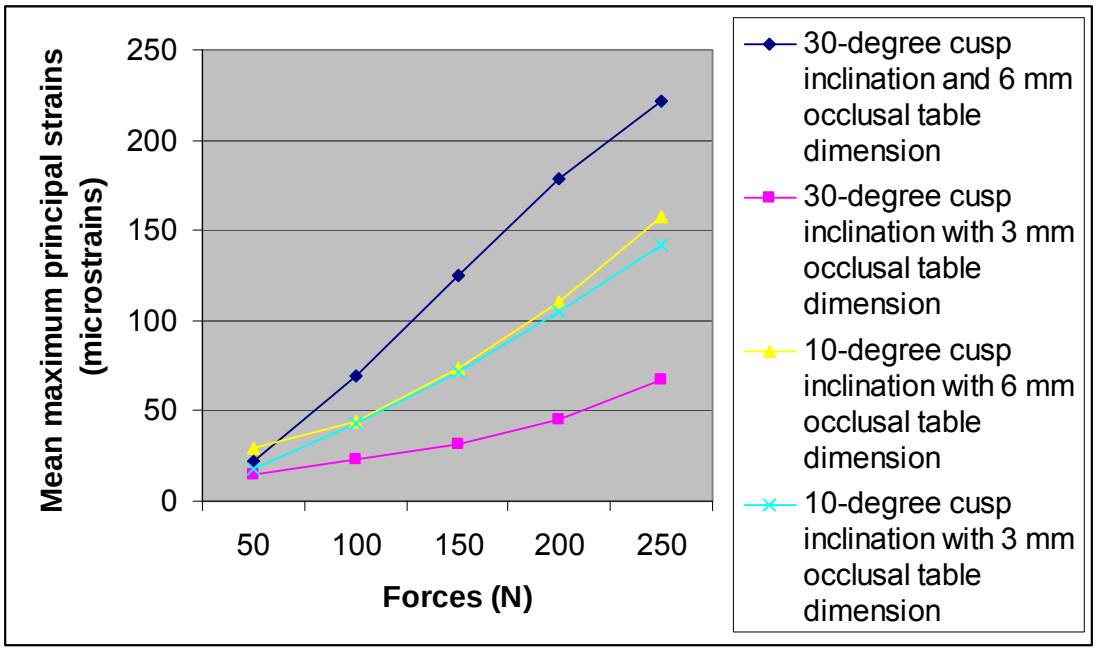

Figure III – 5 Microstrains of four different occlusal design specimens under loading at the central fossa with the strain gauges attached on the buccal side.

The following observations may be made from table III – 3 and figure III – 5:

a) Maximum principal strains (microstrains) increased significantly when the applied series of axial loading was increased from 50 N to 250 N.

b) The highest maximum principal strain (microstrain) of 128.71 was seen in the model one - 30-degree cusp inclination with 6-mm occlusal table dimension, whereas the lowest of 75.82 was seen in the model two - 30-degree cusp inclination with 3-mm occlusal table dimension. The maximum principal strains (microstrains) were defined as a dependent variable, while occlusal designs were defined as a fixed factor.

c) The Univariate Analysis of Variance (ANOVA) with post hoc test comparing the maximum principal strains (microstrains) for the four different occlusal design specimens indicated significant differences in

maximum principal strains (microstrains) between model one, two, three, and four specimens, when an applied axial load was directed at central fossa with strain gauges attached on the buccal side of the bone simulated model ($p = 0.000 – 0.001$).

2.1.4 *Experimental data and analyses for maximum principal strains (microstrains) for four different occlusal design specimens when applied loading at central fossa and strain gauges attached on lingual side.*

Table III – 4 Microstrains of four different occlusal designs under loading at central fossa with strain gauges attached on the lingual side.

Occlusal designs	Cusp inclination	Occlusal table dimension	Forces	Mean maximum principal strains (microstrains)	SD
Model 1	30	6mm	50	37.36	6.22
			100	83.14	13.16
			150	141.81	25.67
			200	185.78	23.71
			250	245.46	33.04
			Total	142.35	72.96
Model 2	30	3mm	50	30.39	10.96
			100	44.70	7.77
			150	61.47	13.03
			200	79.14	12.03
			250	101.14	5.54
			Total	64.82	26.59
Model 3	10	6mm	50	46.85	30.88
			100	75.82	26.56
			150	91.24	42.55
			200	103.49	40.08
			250	115.97	40.24
			Total	88.34	42.66
Model 4	10	3mm	50	69.62	24.67
			100	103.16	37.43
			150	113.66	40.06
			200	172.38	68.82
			250	203.89	57.52
			Total	137.92	69.73

F: 94.96

Occlusal design: model 1 and model 2 (P:0.000), model 1 and model 3 (P:0.000), model 1 and model 4 (P:1.000), model 2 and model 3 (P:0.009), model 2 and model 4 (P:0.000), model 3 and model 4 (P:0.000) (post hoc test)

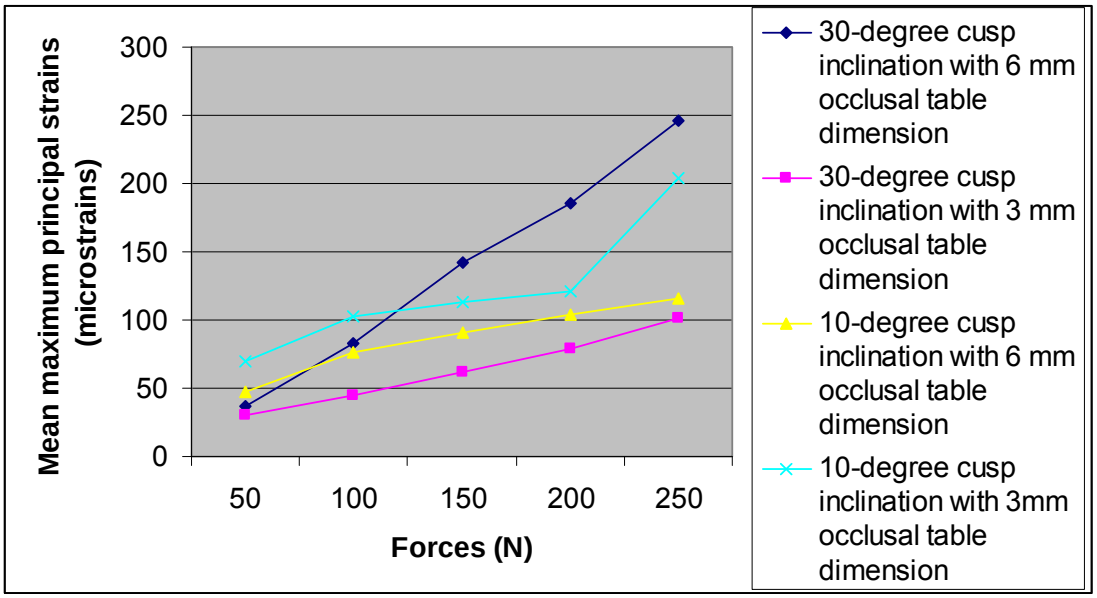

Figure III – 6 Microstrains of four different occlusal design specimens under loading at the central fossa with strain gauges attached on the lingual side.

The following observations may be made from table III – 4 and figure III – 6:

a) Maximum principal strains (microstrains) were increased significantly when the applied series of axial loading was increased from 50 N to 250 N.

b) The highest maximum principal strain (microstrain) of 142.35 was seen in the model one - 30-degree cusp inclination with 6-mm occlusal table dimension, whereas the lowest of 64.82 was seen in the model two - 30-degree cusp inclination with 3-mm occlusal table dimension. The maximum principal strains (microstrains) were defined as a dependent variable, while occlusal designs were defined as a fixed factor.

c) Univariate Analysis of Variance (ANOVA) with post hoc test compared the maximum principal strains (microstrains) for four different occlusal designs. The data indicated significant differences of the maximum principal strains (microstrains) between model one and two; model one

and three; model two and four and model three and four, with applied axial loading at the central fossa and strain gauges attached on lingual side of the bone simulated model (p = 0.000). However, there were no statistically significant differences of the maximum principal strains (microstrains) between model one and four; and model two and three (p = 0.009 - 1.000).

2.1.5 *Experimental data and analyses for the maximum principal strains (microstrains) with 30-degree cusp inclination and 10-degree cusp inclination*

Table III – 5 Mean maximum principal strains (microstrains) of 30-degree cusp inclination specimens and 10-degree cusp inclination specimens

Cusp inclination	Forces	Mean maximum principal strains (microstrains)	SD
30	50	66.03	61.67
	100	152.14	150.49
	150	234.71	240.04
	200	322.07	342.14
	250	383.72	387.91
	Total	240.86	294.20
10	50	40.27	24.19
	100	72.65	31.73
	150	105.20	40.03
	200	150.25	57.23
	250	193.48	68.47
	Total	115.26	72.82

F: 22.108

30-cusp inclination and 10-degree cusp inclination (P:0.000) (univariate test)

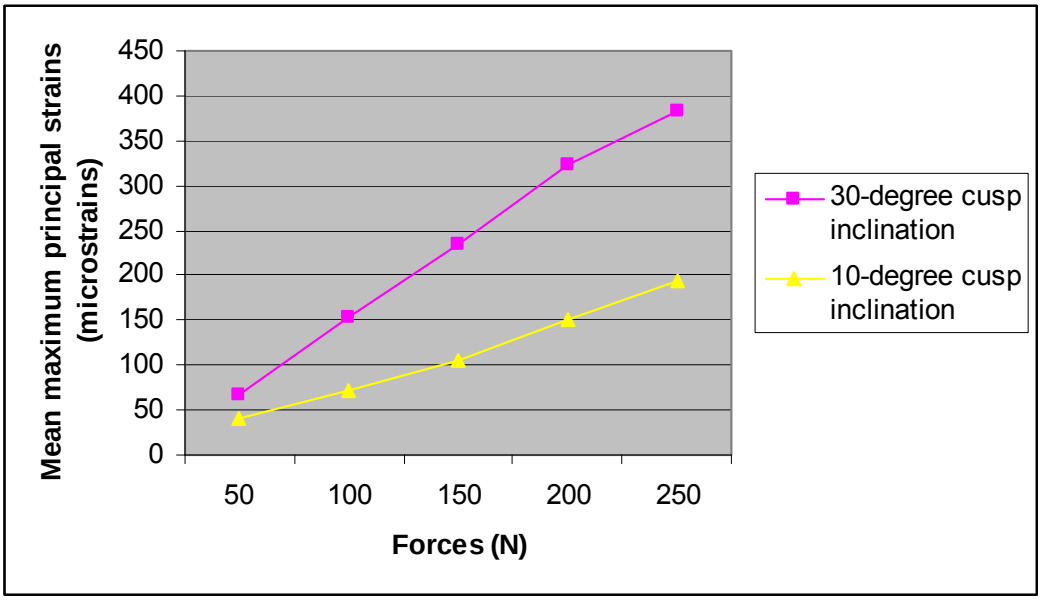

Figure III – 7 Mean maximum principal strains (microstrains) of 30-degree cusp inclination and 10-degree cusp inclination.

The following observations may be made from table III – 5 and figure III – 7:

a) Maximum principal strains (microstrains) were increased significantly when the applied series of axial loading was increased from 50 N to 250 N.

b) In total conditions, mean maximum principal strain (microstrains) of 30-degree cusp inclination specimens (240.86) was significantly higher than that of 10-degree cusp inclination specimens (115.28). The maximum principal strains (microstrains) were defined as a dependent variable, while cusp inclination was defined as a fixed factor.

c) Univariate Analysis of Variance (ANOVA) comparing the maximum principal strains (microstrains) for 30-degree cusp inclination specimens and 10-degree cusp inclination specimens, indicated a significant difference between the two different cusp inclinations ($p = 0.000$).

2.1.6 *Experimental data and analyses for the maximum principal strains (microstrains) with 6-mm occlusal table dimension specimens and 3-mm occlusal table dimension specimens.*

Table III – 6 Mean maximum principal strains (microstrains) of 6-mm occlusal table dimension specimens and 3-mm occlusal table dimension specimens.

Occlusal table dimension	Forces	Mean maximum principal strains (microstrains)	SD
6 mm	50	70.89	61.49
	100	160.34	150.29
	150	251.87	237.98
	200	349.19	334.90
	250	415.76	376.68
	Total	260.50	293.82
3 mm	50	36.80	22.64
	100	68.36	32.44
	150	94.16	42.26
	200	128.55	57.93
	250	164.17	62.69
	Total	100.41	64.59

F: 22.108

6 mm occlusal table dimension and 3 mm occlusal table dimension (P:0.000) (univariate test)

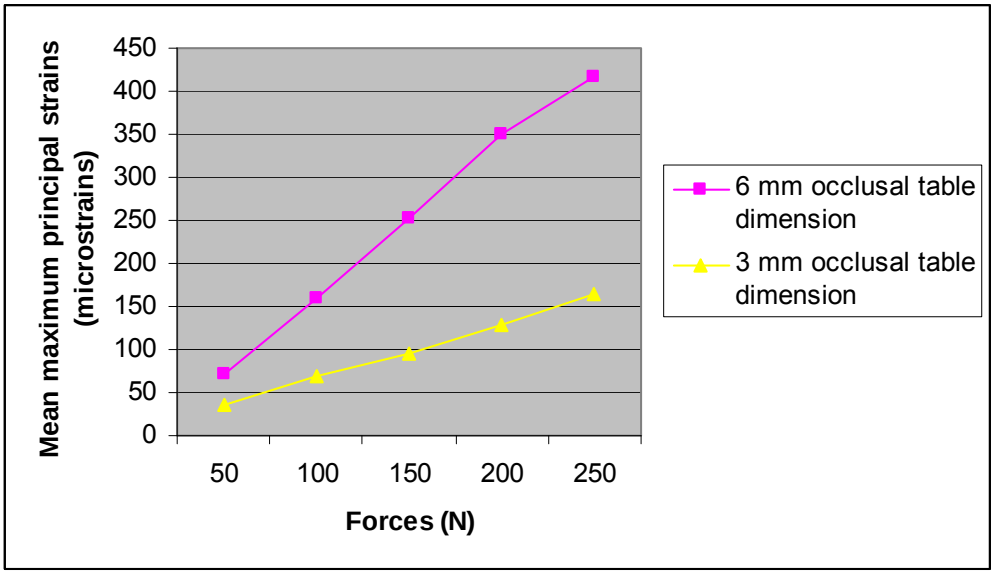

Figure III – 8 Mean maximum principal strains (microstrains) of 30-degree cusp inclination specimens and 10-degree cusp inclination specimens.

The following observations may be made from table III – 6 and figure III – 8:

a) The 6-mm occlusal table dimension specimens had higher mean maximum principal strains (microstrains) on the simulated bone model, compared with the 3-mm occlusal table dimension - 260.50 and 100.41 respectively. The mean maximum principal strains (microstrains) were defined as a dependent variable, while the occlusal table dimension was defined as a fixed factor.

b) Univariate Analysis of Variance (ANOVA) comparing the mean maximum principal strains (microstrains) for the 6- and 3-mm occlusal table dimension specimens, indicated significant differences between the mean maximum principal strains (microstrains) recorded at the cervical area on both sides of the two specimens ($p = 0.000$).

2.2 EFFECT OF THE POSITION OF LOADING

Table III – 7 Mean maximum principal strains (microstrains) of specimens with an applied load at 2 mm buccal on the inclined plane and at the central fossa

Position of loading	Forces	Mean maximum principal strains (microstrains)	SD
2 mm buccal inclined plane	50	69.27	59.21
	100	160.98	145.46
	150	263.01	237.56
	200	365.04	333.75
	250	436.46	376.53
	Total	264.02	292.93
central fossa	50	35.71	23.70
	100	62.90	29.86
	150	89.81	42.31
	200	121.99	58.22
	250	157.82	66.99
	Total	97.73	64.63

F: 29.782

Applied load at 2 mm buccal on the inclined plane and the applied load at the central fossa (P:0.000) (univariate test)

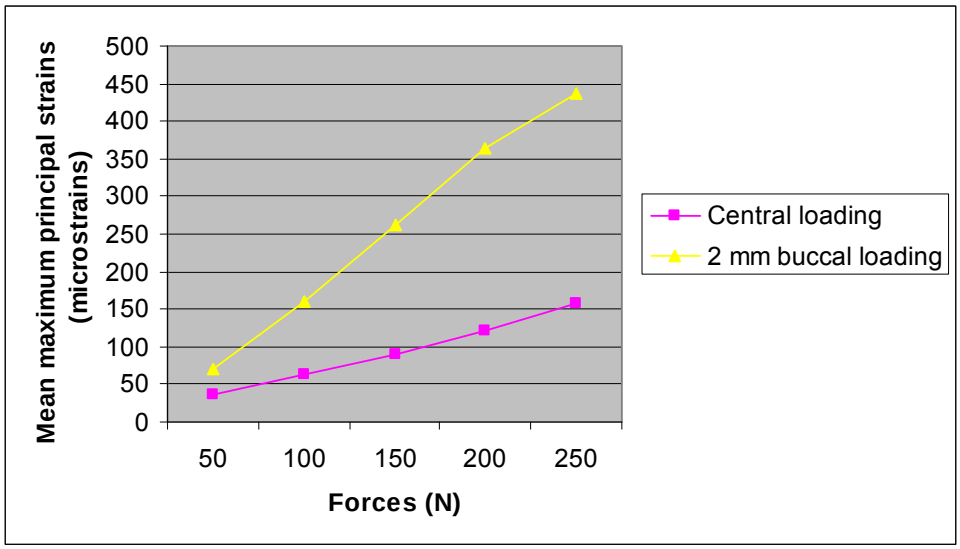

Figure III – 9 Mean maximum principal strains (microstrains) of specimens with an applied load at 2 mm on the buccal inclined plane and at the central fossa.

The following observations may be made from table III – 7 and figure III – 9:

a) The 2 mm buccally loaded specimens had significantly higher mean maximum principal strains (microstrains) on the simulated bone model compared with the central fossa loaded specimens - 264.02 and 97.73 respectively. The maximum principal strains were defined as a dependent variable, while position was defined as a fixed factor.

b) Univariate Analysis of Variance (ANOVA) comparing the mean maximum principal strains (microstrains) for the central and 2 mm buccal positions of occlusal loading indicated significant differences between the mean maximum principal strains recorded at the cervical area of the two specimens (p = 0.000).

2.3 EFFECT OF SIDE MEASUREMENT

Table III – 8 Mean maximum principal strains (microstrains) of specimens with strain gauges attached on the buccal and the lingual sides.

Side measurement	Forces	Mean maximum principal strains (microstrains)	SD
Buccal	50	44.77	46.63
	100	110.92	135.75
	150	189.67	233.06
	200	271.54	333.32
	250	332.57	375.94
	Total	198.53	282.71
Lingual	50	62.09	49.99
	100	117.67	98.16
	150	164.24	137.65
	200	213.41	174.90
	250	255.70	190.81
	Total	166.09	157.13

F: 34.560

Measurement of maximum principal strains on the buccal and lingual sides (P:0.000) (univariate test)

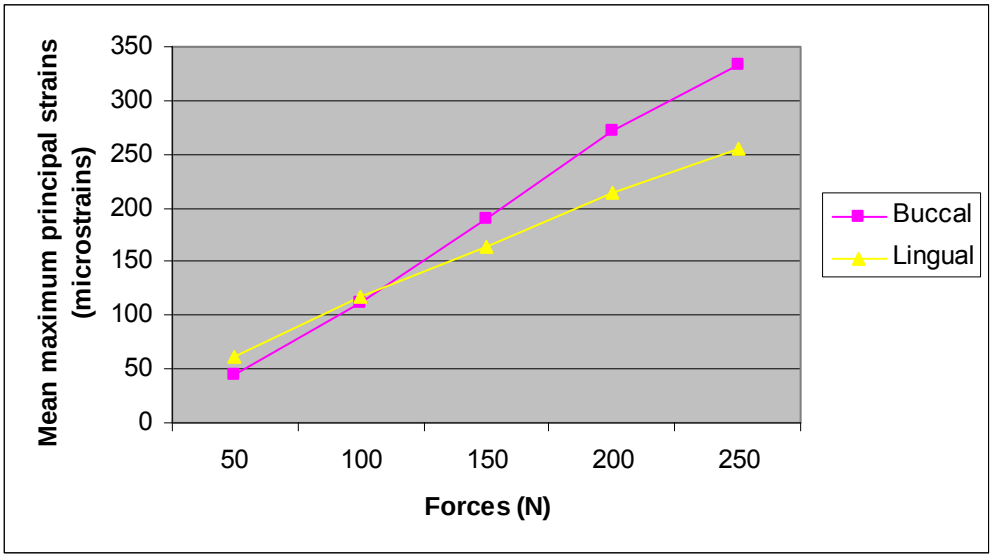

Figure III – 10 Mean maximum principal strains (microstrains) of specimens when measured on the buccal and lingual sides.

The following observations may be made from table III – 8 and figure III – 10:

a) The strains measured on the lingual side had higher mean maximum principal strains (microstrains) than that measured on the buccal side when loading with a force of 50 N. However, there was a reverse trend after increased load of more than 50 N which was significantly different with the mean maximum principal strains (microstrains) of 198.53 and 166.09 on the buccal and lingual areas, respectively. The maximum strains were defined as a dependent variable, while the side was defined as a fixed factor.

b) Univariate Analysis of Variance (ANOVA) comparing the maximum principal strains when measured on the buccal and lingual area of the bone simulation model, indicated a significant difference between the maximum principal strains recorded at the cervical area of the two specimens ($p = 0.000$).

CHAPTER 4

DISCUSSION

This study was designed to provide clinical understanding of the application of quantified axial forces to a prosthetic superstructure and in relation to forces transmitted through four different occlusal designs to a simulated bone model supporting the implant. The data were analysed to compare the maximum principal strains (microstrains), registered by the strain gauges, on the buccal/lingual surface in the cervical area of the simulated bone model. Differences between the two cusp inclinations and two occlusal table dimensions, with considering of other factors, indicated a statistical difference on maximum principal strains as reported in the Results. However, an understanding of the influence of occlusal design on force transmission to implant-supported single crowns and the effect of strain on the simulated bone model need to be discussed.

1. IMPLANT-SUPPORTED SINGLE CROWN MODEL

The model examined implant-supported second premolar single crowns. The simulated bone model can only represent an approximation of the clinical situation, as it is not possible to precisely simulate the morphology and properties of bone which affect the strains on surrounding bone of dental implants. The mechanical properties of the bone simulation model are based on acrylic resin (modulus of elasticity 2.367 GPa), which has slightly different modulus of elasticity as that reported for human dense trabecular bone (1.37 GPa – Ciberka et al., 1992 and Sevimay et al., 2005).

Although the modulus of elasticity of cortical bone (14 GPa – Craig 1980, 1985; Phillips 1990) is five times higher compared with that of acrylic resin, bone-implant contact is mostly within trabeculae bone. To improve the design of a simulated bone model, any material which presents a similar or higher modulus of elasticity to cortical bone should be used around the acrylic resin, to restrict the influence of acrylic resin deformation, and serve as a cortical bone analogue to mimic the real situation. The strain is dependent on the mechanical properties of the materials, so that the applied force may affect different materials differently (Isidor, 2006). That means that the same amount of stress can result in different amount of strain in human bone and acrylic resin. In an attempt to give clinical meaning to the study, the mould of acrylic resin was prepared to a similar shape and size of the human jaw bone in the mandibular premolar area. The bone model was constructed in cross-sectional section, based on the size of a mandible from a CT scan. The size and shape of all simulated bone models were controlled by using a plastic mould.

Osseointegration, as defined by Brånemark et al. (1985), was not achieved in this study. Implants were self-tapped to provide primary stabilisation through the simulated bone model and adaptation was used to simulate in-vitro integration. Maximum stability was confirmed by engaging the entire implant fixture surface with the simulated bone model interface which resulted in an absence of any movements.

The study used ceramic crowns with temporary abutments, which may not often be used in clinical situations. Clinically, porcelain-fused-to-metal crowns or all ceramics crowns are used with gold or titanium abutments in permanent restorations, and acrylic resin crowns may be applied with temporary abutments. However, acrylic resin crowns could not be used in this study because of the yielding or non-linear deformation of the material. Resinous materials would not withstand 250 N occlusal force when loading with a 1-mm crosshead, and ceramic materials have a higher strength compared with resinous materials. Moreover, with the use of CAD/CAM technology, ceramic crowns could be milled and duplicated to the exact size and shape to ensure standardize crown accuracy.

2. THE EXPERIMENTAL PROCEDURE

Attempts were made to simulate in the in-vitro study, as closely as possible, the range of conditions applied and occurring in the oral cavity.

The axis of the implant fixture was prepared perpendicular to the bone simulation model to confirm an axial force direction. Only axial forces with static loads were applied in this study. Although animal experimental studies indicated that high cyclic loads have a more detrimental effect on the bone around dental implants than static loads (Duyck, 2001, Gotfredsen et al., 2001 and 2002), axial forces with static loads in this study were assumed to duplicate sustained forces such as with clenching, as a component of masticatory function.

The elasticity of the food bolus also has an impact on the resultant forces distributed to the teeth. The study by Wang and Stohler (1990) reported that each test food has particular textural properties reflected in characteristic details of its force-time curves. The degree of horizontal forces would be affected by the consistency of the bolus. For example, tough foods require more occlusal force, and occlusal force is distributed to the superstructure and dental implants as if the cuspal inclines were in contact. The direction of that resultant is perpendicular to the cuspal inclination.

Cyclic loads and food consistency were not taking into account in this study, as the study aimed to investigate the effect of occlusal designs in relation to the deflection on the bone simulated model with control of variables that could affect on the results. However, it would be more realistic to apply cyclic loads with or without considering the elasticity of the bolus of foods to more accurately simulate the oral environment in an in-vitro study.

Location of the attachment for the strain gauges was important because the strains were measured only at the point where the strain gauges were attached. In this study, the location of the attachment of the strain gauges was specifically on the buccal and lingual sides in the cervical area of the bone simulation model. The sloped area as mentioned in chapter two, which was referred to the buccal and lingual side of the bone simulated model, was divided into 9 parts. The middle part was selected to attach the strain gauges. The location of the attachment site in this region was based on a preliminary finite element analysis, animal experiments and clinical

observations that excessive loading of implant-supported restorations was reported to induce marginal bone resorption along the neck of the implants (Duyck, 2001; Naert, 2001a-b and Brunski, 2000). Although the location of the strain gauges was not exactly on the neck of the implant, the attachment position in this study was the closest to the maximum peak stress position, that was able to support the strain gauges.

The applied forces were loaded on two loading sites, the central area and 2 mm buccal along the cusp from in the middle of the occlusal table of each specimen, which defined loading position and line of loading. In this study, the crosshead distance was manually controlled by a handle. A ruler was used to measure the distance from the centre to the 2 mm buccal position.

3. ANALYSIS OF THE DATA

The applied forces quantified by the compression load cell of the universal testing machine and the microstrains registered by the rosette strain gauges demonstrated inconsistent values with a moderate range of standard deviation. The inconsistent data may be due to the strain gauges, which were sensitive to temperature, and slight errors of the loading position may have affected the microstrain values. Specimen sizes and methodology were standardised.

To analyse the data with inconsistent values and a moderate range of SD, box plots were used. Any outliers were removed, and the analysis was then

conducted with Univariate Analysis of Variance (ANOVA) with Bonferroni as the post- hoc adjustment for multiple comparisons.

Loading on the central area of the occlusal specimens caused a significant difference in mean maximum principal strains (97.73 microstrains) compared with the 2-mm buccal loading of the occlusal specimens (264.02 microstrains). This is in agreement with several studies (Rangert, 1997; Weinberg,1995 and 1998), which recommended that the optimal transfer of vertical occlusal load through an implant is along the implant's long-axis, to decrease bending moments created within the implant.

There was also a significant difference in the mean maximum principal strains (microstrains) of the buccal area of the simulated bone model (198.53) compared to that of the lingual area of the simulated bone model (166.09). It may be assumed that strains occurred on the ipsilateral side of the occlusal loading.

When an applied axial load at 2 mm buccal along the inclined plane of the cusp and with strain gauges attached on the buccal side of the simulated bone model, the highest mean maximum principal strain (811.52 microstrains) was seen in the model one (30-degree cusp inclination with 6-mm occlusal table dimension), followed by model three (10-degree cusp inclination with 6- mm occlusal table dimension), then model two (30-degree cusp inclination with 3-mm occlusal table dimension), and model four (10-degree cusp inclination with 3-mm occlusal table dimension). The respective

microstrains were 177.40, 141.32 and 75.30 microstrains. This agrees with the report of Kaukinen et al. (1996) that the initial breakage force for the higher degree cusped occlusal design was greater than the initial breakage for the cuspless occlusal design specimens, although in that study no significance was demonstrated in maximum strain between 33-degree cusped and 0-degree cuspless occlusal designs. Morneburg and Pröschel (2003) also supported that narrowing the bucco-lingual width of the occlusal surface by 30% and chewing soft food significantly reduced bending moments on posterior three-unit fixed prostheses. The two important factors, reduced inclination of tooth cusps and a narrowed occlusal table, are the occlusal designs recommended by several studies (Klineberg et al., 2007; Kim et al., 2005; Stanford, 2005; Curtis et al., 2000; Weinberg, 1995 and 1998). Although proprioception and muscle programming possibly limit high occlusal forces, overload through restorations on dental implants can be minimized by reducing horizontal forces, which cause bending and overload.

Statistical differences were also indicated between the maximum principal strains (microstrains) of the occlusal design model one, two, three, and four specimens when applied an axial loading at 2 mm buccal inclined plane and strain gauges attached on buccal side of simulated bone model. The maximum principal strains were higher in the model one and three, which both had the 6-mm occlusal table dimension irrespective of the cusp inclinations. This result is in agreement with Morneburg and Pröschel (2003). From this study, the occlusal table dimension seems to play a more important role than cusp inclination, although the cusp inclination is still a

factor to be considered. Moreover, combination of the two factors, cusp inclination and occlusal table dimension, significantly affects the magnitude of forces transmitted to implant-supported prostheses.

Bone remodeling is a surface-specific phenomenon that occurs during growth as part of wound healing and in response to bone loading. Ideal restorations can promote positive bone remodeling and also minimize the healing time. Superstructure designs of dental implants, especially occlusal designs, may have an impact on bone strains around dental implants when occlusal loads are applied. As mentioned in literature review, bone tissue reacts to strain (i.e., deformation). Bone is believed to function within the strain range of approximately 50 – 1500 microstrains (Frost, 2004). If the strain in the bone surrounding dental implants is in the 'mild overload' range (1500–3000 microstrain), apposition of bone seems to be the biological response (Forst, 2004 and Isidor, 2006). The highest mean maximum principal strains (811.52 microstrains) from the model one, with the range from 163.43 to 1258.89 microstrains, and the lowest mean maximum principal strains (75.30 microstrains) from the model four, with the range from 5.10 to 156.98 microstrains, were obtained. These values of microstrains are still in a range of bone function, regardless of cusp inclination and occlusal table dimension. However, the influence of strain values in this study cannot be considered as bone remodeling depends on several factors. Firstly, in this study, the properties and morphology of the simulated bone model is not identical to the properties of human bone. Even human bone properties still vary individually. Moreover, the experimental

models were not osseointegrated clinically; thus forces cannot be assumed to be transferred directly across the implant-bone interface. Finally, the location of strain gauges was also slightly away from the point of maximum peak stress. The maximum principal strains (microstrains) on the simulated bone would be affected by these factors.

However, the rational for investigating parameters regarding superstructure designs on dental implants is based on the idea of predicting the best design for treatment options. Strain values in six channels, measuring from the attached strain gauges, were balanced at zero before applied occlusal loading on the superstructure of specimens. Therefore, the calculated maximum principal strain (microstrains) in each occlusal design specimen could be represented as principal maximum strains recorded for the specific simulated implant-supported single crown models. The results from this study suggest that cusp inclination and occlusal table dimension significantly affect the magnitude of forces transmitted to implant-supported prostheses, which would have an effect on surrounding bone strains of dental implants when occlusal loads are applied in the clinical situations. The specific occlusal designs, as a prototype to promote positive bone remodeling and also minimize the healing time, is still a challenge for future researches to provide more clinical understanding on the role of superstructure occlusal designs to stress / strain distributions in relation to bone remodeling.

CHAPTER 5

CONCLUSION

This study used the method of applying quantified axial forces to an implant and recording the forces transmitted through four different occlusal designs to a simulated bone model supporting the implant. The data were analysed to compare the maximum principal strains (microstrains), registered by the strain gauges, on the buccal/lingual surfaces in the cervical areas of the simulated bone model. It is not appropriate to draw a firm conclusion about the clinical significance of this study, but within the study limitations and based on strain gauge analysis, the following conclusions can be drawn:

1. Statistical differences were demonstrated in maximum principal strains (microstrain) between the 30-degree cusped and the 0-degree cusp inclination specimens, and the 6-mm occlusal table dimension and the 3-mm occlusal table dimension specimens.
2. Combination of the two factors, cusp inclination and occlusal table dimension, significantly affects the magnitude of forces transmitted to implant-supported prostheses. This leads to a higher maximum principal strain (microstrains) on the simulated bone model.
3. Occlusal table dimensions seem to play a more important role than cusp inclination, and loading on the central area of the occlusal table exhibited a significant difference in maximum principal strains (microstrains) compared with the 2-mm buccal loading of occlusal specimens.
4. Maximum strain occurred on the ipsilateral side of occlusal loading.

APPENDICES

Tables 1-20 demonstrate the maximum strains for 30-degree and 10-degree cusp inclination and 3- and 6-mm occlusal table dimension specimens registered by strain gauges.

1. Table of data deflection: 30-degree cusp inclination, 6-mm occlusal table dimension, with an axial loading of 50N

Table 1

Test	Position of loading	Side of deflection on bone model	Maximum strain	Test	Position of loading	Side of deflection on bone model	Maximum strain
1	central	buccal	14.22874	1	central	lingual	40.51461
2	central	buccal	30.6869	2	central	lingual	37.6987
3	central	buccal	36.51424	3	central	lingual	46.14401
4	central	buccal	15.29849	4	central	lingual	36.45284
5	central	buccal	26.70374	5	central	lingual	70.05635
6	central	buccal	22.56231	6	central	lingual	28.11615
7	central	buccal	16.0825	7	central	lingual	42.42087
8	central	buccal	28.57357	8	central	lingual	56.63923
9	central	buccal	20.94211	9	central	lingual	38.55228
10	central	buccal	18.10182	10	central	lingual	28.94131
1	2 mm	buccal	92.55271	1	2 mm	lingual	40.51461
2	2 mm	buccal	70.56461	2	2 mm	lingual	37.6987
3	2 mm	buccal	151.8914	3	2 mm	lingual	46.14401
4	2 mm	buccal	141.1163	4	2 mm	lingual	36.45284
5	2 mm	buccal	154.8184	5	2 mm	lingual	70.05635
6	2 mm	buccal	172.1744	6	2 mm	lingual	28.11615
7	2 mm	buccal	160.7339	7	2 mm	lingual	42.42087
8	2 mm	buccal	191.6894	8	2 mm	lingual	56.63923
9	2 mm	buccal	171.6034	9	2 mm	lingual	38.55228
10	2 mm	buccal	208.0265	10	2 mm	lingual	28.94131

2. Table of data deflection: 30-degree cusp inclination, 6-mm occlusal table dimension, with an axial loading of 100 N

Table 2

Test	Position of loading	Side of deflection on bone model	Maximum strain	Test	Position of loading	Side of deflection on bone model	Maximum strain
1	central	buccal	52.90877	1	central	lingual	107.6013
2	central	buccal	80.9902	2	central	lingual	97.41048
3	central	buccal	91.89788	3	central	lingual	79.54546
4	central	buccal	54.38518	4	central	lingual	79.67161
5	central	buccal	79.57847	5	central	lingual	130.883
6	central	buccal	68.82839	6	central	lingual	71.44499
7	central	buccal	64.03445	7	central	lingual	84.71371
8	central	buccal	85.44879	8	central	lingual	117.0577
9	central	buccal	67.86332	9	central	lingual	69.56144
10	central	buccal	66.45749	10	central	lingual	75.18529
1	2 mm	buccal	312.7088	1	2 mm	lingual	294.41
2	2 mm	buccal	333.1416	2	2 mm	lingual	284.2046
3	2 mm	buccal	446.5983	3	2 mm	lingual	306.9172
4	2 mm	buccal	453.3229	4	2 mm	lingual	334.5576
5	2 mm	buccal	474.3217	5	2 mm	lingual	387.5915
6	2 mm	buccal	478.7287	6	2 mm	lingual	336.8508
7	2 mm	buccal	462.253	7	2 mm	lingual	358.2597
8	2 mm	buccal	509.1146	8	2 mm	lingual	380.4481
9	2 mm	buccal	486.5469	9	2 mm	lingual	406.3221
10	2 mm	buccal	538.335	10	2 mm	lingual	380.1276

3. Table of data deflection: 30-degree cusp inclination, 6-mm occlusal table dimension, with an axial loading of 150 N

Table 3

Test	Position of loading	Side of deflection on bone model	Maximum strain	Test	Position of loading	Side of deflection on bone model	Maximum strain
1	central	buccal	94.68463	1	central	lingual	162.6662
2	central	buccal	132.7018	2	central	lingual	159.4824
3	central	buccal	150.2371	3	central	lingual	115.1351
4	central	buccal	108.2365	4	central	lingual	130.9807
5	central	buccal	136.0204	5	central	lingual	190.8178
6	central	buccal	116.9857	6	central	lingual	123.8177
7	central	buccal	118.7106	7	central	lingual	125.3736
8	central	buccal	155.9371	8	central	lingual	165.2163
9	central	buccal	118.158	9	central	lingual	117.3181
10	central	buccal	122.5365	10	central	lingual	127.2518
1	2 mm	buccal	540.3543	1	2 mm	lingual	389.6668
2	2 mm	buccal	672.0055	2	2 mm	lingual	441.5236
3	2 mm	buccal	830.0485	3	2 mm	lingual	476.9881
4	2 mm	buccal	790.1053	4	2 mm	lingual	508.2164
5	2 mm	buccal	801.7937	5	2 mm	lingual	546.4664
6	2 mm	buccal	782.3239	6	2 mm	lingual	472.7292
7	2 mm	buccal	751.0767	7	2 mm	lingual	518.797
8	2 mm	buccal	788.9674	8	2 mm	lingual	505.3315
9	2 mm	buccal	769.8453	9	2 mm	lingual	559.1521
10	2 mm	buccal	786.653	10	2 mm	lingual	483.1657

4. Table of data deflection: 30-degree cusp inclination, 6-mm occlusal table dimension, with an axial loading of 200 N

Table 4

Test	Position of loading	Side of deflection on bone model	Maximum strain	Test	Position of loading	Side of deflection on bone model	Maximum strain
1	central	buccal	158.3173	1	central	lingual	203.0424
2	central	buccal	178.5707	2	central	lingual	226.1714
3	central	buccal	195.0051	3	central	lingual	164.7864
4	central	buccal	156.9145	4	central	lingual	179.9786
5	central	buccal	195.877	5	central	lingual	244.7288
6	central	buccal	168.4506	6	central	lingual	153.9049
7	central	buccal	168.4485	7	central	lingual	180.4282
8	central	buccal	217.2168	8	central	lingual	210.998
9	central	buccal	167.8891	9	central	lingual	165.4675
10	central	buccal	174.5121	10	central	lingual	187.2804
1	2 mm	buccal	996.2154	1	2 mm	lingual	567.7038
2	2 mm	buccal	1094.95	2	2 mm	lingual	639.8197
3	2 mm	buccal	1127.413	3	2 mm	lingual	622.736
4	2 mm	buccal	1128.682	4	2 mm	lingual	659.4049
5	2 mm	buccal	1130.068	5	2 mm	lingual	682.2914
6	2 mm	buccal	1108.249	6	2 mm	lingual	619.6158
7	2 mm	buccal	1095.846	7	2 mm	lingual	694.1992
8	2 mm	buccal	1086.567	8	2 mm	lingual	640.889
9	2 mm	buccal	1026.772	9	2 mm	lingual	699.2664
10	2 mm	buccal	1082.851	10	2 mm	lingual	622.9195

5. Table of data deflection: 30-degree cusp inclination, 6-mm occlusal table dimension, with an axial loading of 250 N

Table 5

Test	Position of loading	Side of deflection on bone model	Maximum strain	Test	Position of loading	Side of deflection on bone model	Maximum strain
1	central	buccal	202.6049	1	central	lingual	270.8616
2	central	buccal	234.186	2	central	lingual	284.794
3	central	buccal	229.9779	3	central	lingual	217.1735
4	central	buccal	198.4608	4	central	lingual	210.112
5	central	buccal	244.404	5	central	lingual	296.8386
6	central	buccal	208.8418	6	central	lingual	189.6031
7	central	buccal	210.8834	7	central	lingual	233.3099
8	central	buccal	264.6887	8	central	lingual	237.126
9	central	buccal	207.6424	9	central	lingual	205.7302
10	central	buccal	212.7475	10	central	lingual	253.1608
1	2 mm	buccal	1284.397	1	2 mm	lingual	692.9472
2	2 mm	buccal	1264.353	2	2 mm	lingual	717.6732
3	2 mm	buccal	1281.272	3	2 mm	lingual	693.3977
4	2 mm	buccal	1252.455	4	2 mm	lingual	759.5477
5	2 mm	buccal	1252.455	5	2 mm	lingual	759.5477
6	2 mm	buccal	1262.209	6	2 mm	lingual	688.5488
7	2 mm	buccal	1246.367	7	2 mm	lingual	784.9943
8	2 mm	buccal	1258.216	8	2 mm	lingual	730.7953
9	2 mm	buccal	1248.122	9	2 mm	lingual	825.0371
10	2 mm	buccal	1240.012	10	2 mm	lingual	706.0319

6. Table of data deflection: 30-degree cusp inclination, 3-mm occlusal table dimension, with an axial loading of 50 N

Table 6

Test	Position of loading	Side of deflection on bone model	Maximum strain	Test	Position of loading	Side of deflection on bone model	Maximum strain
1	central	buccal	-13.588	1	central	lingual	23.35562
2	central	buccal	56.60906	2	central	lingual	61.01804
3	central	buccal	33.42326	3	central	lingual	37.91297
4	central	buccal	4.813526	4	central	lingual	36.33041
5	central	buccal	21.79935	5	central	lingual	38.0436
6	central	buccal	10.78942	6	central	lingual	16.48809
7	central	buccal	4.722542	7	central	lingual	25.36378
8	central	buccal	11.9544	8	central	lingual	3.320006
9	central	buccal	50.25128	9	central	lingual	47.13657
10	central	buccal	-3.3501	10	central	lingual	18.4624
1	2 mm	buccal	43.17278	1	2 mm	lingual	55.08821
2	2 mm	buccal	50.81388	2	2 mm	lingual	54.97528
3	2 mm	buccal	48.49494	3	2 mm	lingual	57.26338
4	2 mm	buccal	47.47307	4	2 mm	lingual	54.59022
5	2 mm	buccal	35.04123	5	2 mm	lingual	35.46081
6	2 mm	buccal	37.55034	6	2 mm	lingual	53.55815
7	2 mm	buccal	48.58974	7	2 mm	lingual	60.71587
8	2 mm	buccal	41.24559	8	2 mm	lingual	44.19363
9	2 mm	buccal	36.89205	9	2 mm	lingual	52.41885
10	2 mm	buccal	36.43643	10	2 mm	lingual	41.84496

7. Table of data deflection: 30-degree cusp inclination, 3-mm occlusal table dimension, with an axial loading of 100 N

Table 7

Test	Position of loading	Side of deflection on bone model	Maximum strain	Test	Position of loading	Side of deflection on bone model	Maximum strain
1	central	buccal	1.532157	1	central	lingual	42.71601
2	central	buccal	-1.27733	2	central	lingual	74.30474
3	central	buccal	-13.6246	3	central	lingual	54.24345
4	central	buccal	-3.66537	4	central	lingual	44.46847
5	central	buccal	-3.99148	5	central	lingual	51.96335
6	central	buccal	38.54337	6	central	lingual	34.19296
7	central	buccal	22.79068	7	central	lingual	43.42813
8	central	buccal	32.61308	8	central	lingual	14.87174
9	central	buccal	9.164337	9	central	lingual	52.23533
10	central	buccal	10.4909	10	central	lingual	34.39018
1	2 mm	buccal	83.95594	1	2 mm	lingual	93.55135
2	2 mm	buccal	98.84687	2	2 mm	lingual	95.28714
3	2 mm	buccal	97.52726	3	2 mm	lingual	98.1436
4	2 mm	buccal	94.78902	4	2 mm	lingual	91.32017
5	2 mm	buccal	83.97413	5	2 mm	lingual	79.16192
6	2 mm	buccal	95.87714	6	2 mm	lingual	94.52704
7	2 mm	buccal	98.49908	7	2 mm	lingual	101.8287
8	2 mm	buccal	89.89479	8	2 mm	lingual	87.38663
9	2 mm	buccal	97.11808	9	2 mm	lingual	98.4642
10	2 mm	buccal	90.5047	10	2 mm	lingual	86.46739

8. Table of data deflection: 30-degree cusp inclination, 3-mm occlusal table dimension, with an axial loading of 150 N

Table 8

Test	Position of loading	Side of deflection on bone model	Maximum strain	Test	Position of loading	Side of deflection on bone model	Maximum strain
1	central	buccal	25.64921	1	central	lingual	56.95728
2	central	buccal	-6.38543	2	central	lingual	87.46308
3	central	buccal	-11.5862	3	central	lingual	65.3646
4	central	buccal	13.12353	4	central	lingual	56.73253
5	central	buccal	7.327949	5	central	lingual	71.52445
6	central	buccal	66.24372	6	central	lingual	58.90327
7	central	buccal	39.45372	7	central	lingual	65.13183
8	central	buccal	55.42989	8	central	lingual	38.95245
9	central	buccal	5.525199	9	central	lingual	64.78753
10	central	buccal	36.22012	10	central	lingual	48.9258
1	2 mm	buccal	124.6925	1	2 mm	lingual	132.6835
2	2 mm	buccal	152.7649	2	2 mm	lingual	134.9446
3	2 mm	buccal	151.0613	3	2 mm	lingual	140.5388
4	2 mm	buccal	139.6847	4	2 mm	lingual	133.1701
5	2 mm	buccal	142.824	5	2 mm	lingual	121.1798
6	2 mm	buccal	153.936	6	2 mm	lingual	136.2539
7	2 mm	buccal	160.0783	7	2 mm	lingual	149.7022
8	2 mm	buccal	146.5512	8	2 mm	lingual	130.8369
9	2 mm	buccal	151.2815	9	2 mm	lingual	143.3589
10	2 mm	buccal	141.4964	10	2 mm	lingual	129.7116

9. Table of data deflection: 30-degree cusp inclination, 3-mm occlusal table dimension, with an axial loading of 200 N

Table 9

Test	Position of loading	Side of deflection on bone model	Maximum strain	Test	Position of loading	Side of deflection on bone model	Maximum strain
1	central	buccal	48.04791	1	central	lingual	76.3407
2	central	buccal	10.37778	2	central	lingual	95.95041
3	central	buccal	8.313878	3	central	lingual	89.22255
4	central	buccal	35.93461	4	central	lingual	78.07401
5	central	buccal	27.01463	5	central	lingual	84.43791
6	central	buccal	87.20218	6	central	lingual	82.93204
7	central	buccal	62.09152	7	central	lingual	83.94652
8	central	buccal	81.52344	8	central	lingual	52.64422
9	central	buccal	22.89402	9	central	lingual	80.56866
10	central	buccal	63.69016	10	central	lingual	67.2364
1	2 mm	buccal	176.0448	1	2 mm	lingual	168.106
2	2 mm	buccal	192.5262	2	2 mm	lingual	174.1631
3	2 mm	buccal	195.9149	3	2 mm	lingual	179.7504
4	2 mm	buccal	187.5506	4	2 mm	lingual	171.5826
5	2 mm	buccal	185.5788	5	2 mm	lingual	162.4029
6	2 mm	buccal	206.1867	6	2 mm	lingual	177.0294
7	2 mm	buccal	200.7619	7	2 mm	lingual	189.927
8	2 mm	buccal	189.6588	8	2 mm	lingual	171.5609
9	2 mm	buccal	201.4562	9	2 mm	lingual	179.4306
10	2 mm	buccal	190.9041	10	2 mm	lingual	170.4229

10. Table of data deflection: 30-degree cusp inclination, 3-mm occlusal table dimension, with an axial loading of 250 N

Table 10

Test	Position of loading	Side of deflection on bone model	Maximum strain	Test	Position of loading	Side of deflection on bone model	Maximum strain
1	central	buccal	80.00628	1	central	lingual	101.7075
2	central	buccal	31.58506	2	central	lingual	109.9856
3	central	buccal	27.98043	3	central	lingual	104.3008
4	central	buccal	55.19934	4	central	lingual	95.00587
5	central	buccal	46.94951	5	central	lingual	100.7212
6	central	buccal	111.938	6	central	lingual	103.9124
7	central	buccal	85.95634	7	central	lingual	103.831
8	central	buccal	98.85453	8	central	lingual	79.73332
9	central	buccal	47.73405	9	central	lingual	99.76662
10	central	buccal	91.12072	10	central	lingual	91.01645
1	2 mm	buccal	227.9814	1	2 mm	lingual	196.2702
2	2 mm	buccal	232.5032	2	2 mm	lingual	211.7564
3	2 mm	buccal	228.0525	3	2 mm	lingual	213.9304
4	2 mm	buccal	226.6264	4	2 mm	lingual	208.1478
5	2 mm	buccal	223.5539	5	2 mm	lingual	194.2503
6	2 mm	buccal	236.5505	6	2 mm	lingual	215.3785
7	2 mm	buccal	239.7122	7	2 mm	lingual	225.8108
8	2 mm	buccal	241.9545	8	2 mm	lingual	208.8438
9	2 mm	buccal	234.0663	9	2 mm	lingual	213.4644
10	2 mm	buccal	227.5266	10	2 mm	lingual	205.8456

11. Table of data deflection: 10-degree cusp inclination, 6-mm occlusal table dimension, with an axial loading of 50 N

Table 11

Test	Position of loading	Side of deflection on bone model	Maximum strain	Test	Position of loading	Side of deflection on bone model	Maximum strain
1	central	buccal	155.4354	1	central	lingual	116.9347
2	central	buccal	57.4706	2	central	lingual	61.78507
3	central	buccal	33.56853	3	central	lingual	15.39999
4	central	buccal	14.32268	4	central	lingual	10.20471
5	central	buccal	13.4799	5	central	lingual	19.46073
6	central	buccal	155.8574	6	central	lingual	122.8597
7	central	buccal	71.06904	7	central	lingual	69.03646
8	central	buccal	60.90543	8	central	lingual	65.49605
9	central	buccal	127.6187	9	central	lingual	92.95179
10	central	buccal	97.72116	10	central	lingual	86.57066
1	2 mm	buccal	44.98487	1	2 mm	lingual	50.44158
2	2 mm	buccal	45.86643	2	2 mm	lingual	35.58683
3	2 mm	buccal	45.51924	3	2 mm	lingual	35.54227
4	2 mm	buccal	43.50684	4	2 mm	lingual	4.043347
5	2 mm	buccal	51.40925	5	2 mm	lingual	28.47886
6	2 mm	buccal	50.87614	6	2 mm	lingual	91.36245
7	2 mm	buccal	49.52334	7	2 mm	lingual	29.76405
8	2 mm	buccal	46.13012	8	2 mm	lingual	41.968
9	2 mm	buccal	50.80836	9	2 mm	lingual	44.95634
10	2 mm	buccal	52.8456	10	2 mm	lingual	37.60365

12. Table of data deflection: 10-degree cusp inclination, 6-mm occlusal table dimension, with an axial loading of 100 N

Table 12

Test	Position of loading	Side of deflection on bone model	Maximum strain	Test	Position of loading	Side of deflection on bone model	Maximum strain
1	central	buccal	167.0111	1	central	lingual	164.3448
2	central	buccal	36.53742	2	central	lingual	58.04785
3	central	buccal	42.52057	3	central	lingual	34.80618
4	central	buccal	49.07654	4	central	lingual	10.62422
5	central	buccal	42.3787	5	central	lingual	18.19108
6	central	buccal	127.0869	6	central	lingual	144.8509
7	central	buccal	37.92352	7	central	lingual	81.38617
8	central	buccal	39.85333	8	central	lingual	74.34889
9	central	buccal	89.94839	9	central	lingual	103.0672
10	central	buccal	61.91254	10	central	lingual	103.2822
1	2 mm	buccal	92.25687	1	2 mm	lingual	99.06678
2	2 mm	buccal	102.1441	2	2 mm	lingual	70.02939
3	2 mm	buccal	101.2369	3	2 mm	lingual	79.64955
4	2 mm	buccal	101.0368	4	2 mm	lingual	46.91621
5	2 mm	buccal	110.986	5	2 mm	lingual	67.89761
6	2 mm	buccal	105.4216	6	2 mm	lingual	152.8557
7	2 mm	buccal	104.3242	7	2 mm	lingual	77.38621
8	2 mm	buccal	105.8983	8	2 mm	lingual	83.78106
9	2 mm	buccal	106.5676	9	2 mm	lingual	88.61786
10	2 mm	buccal	172.1385	10	2 mm	lingual	123.9192

13. Table of data deflection: 10-degree cusp inclination, 6-mm occlusal table dimension, with an axial loading of 150 N

Table 13

Test	Position of loading	Side of deflection on bone model	Maximum strain	Test	Position of loading	Side of deflection on bone model	Maximum strain
1	central	buccal	105.7263	1	central	lingual	197.3623
2	central	buccal	72.1531	2	central	lingual	69.17513
3	central	buccal	79.77357	3	central	lingual	44.85612
4	central	buccal	87.575	4	central	lingual	23.97528
5	central	buccal	81.74613	5	central	lingual	30.33629
6	central	buccal	88.99943	6	central	lingual	157.7841
7	central	buccal	63.32351	7	central	lingual	92.23106
8	central	buccal	77.43808	8	central	lingual	92.87055
9	central	buccal	52.2944	9	central	lingual	114.856
10	central	buccal	55.20985	10	central	lingual	127.8121
1	2 mm	buccal	157.7476	1	2 mm	lingual	154.7317
2	2 mm	buccal	163.5272	2	2 mm	lingual	125.7476
3	2 mm	buccal	162.8932	3	2 mm	lingual	125.3595
4	2 mm	buccal	166.3188	4	2 mm	lingual	98.71051
5	2 mm	buccal	176.5687	5	2 mm	lingual	123.4402
6	2 mm	buccal	173.8393	6	2 mm	lingual	197.0162
7	2 mm	buccal	166.2263	7	2 mm	lingual	120.197
8	2 mm	buccal	169.3997	8	2 mm	lingual	128.1529
9	2 mm	buccal	168.9931	9	2 mm	lingual	134.3844
10	2 mm	buccal	241.9105	10	2 mm	lingual	171.272

14. Table of data deflection: 10-degree cusp inclination, 6-mm occlusal table dimension, with an axial loading of 200 N

Table 14

Test	Position of loading	Side of deflection on bone model	Maximum strain	Test	Position of loading	Side of deflection on bone model	Maximum strain
1	central	buccal	108.5658	1	central	lingual	194.7045
2	central	buccal	117.9335	2	central	lingual	81.63008
3	central	buccal	123.6384	3	central	lingual	55.7192
4	central	buccal	131.1776	4	central	lingual	31.92947
5	central	buccal	125.439	5	central	lingual	49.99131
6	central	buccal	84.70554	6	central	lingual	169.9768
7	central	buccal	106.3589	7	central	lingual	103.3089
8	central	buccal	120.3197	8	central	lingual	115.7187
9	central	buccal	84.9892	9	central	lingual	120.254
10	central	buccal	95.37251	10	central	lingual	131.3532
1	2 mm	buccal	246.8487	1	2 mm	lingual	248.3186
2	2 mm	buccal	237.2776	2	2 mm	lingual	165.6137
3	2 mm	buccal	235.6125	3	2 mm	lingual	166.9189
4	2 mm	buccal	237.4547	4	2 mm	lingual	143.4613
5	2 mm	buccal	251.7614	5	2 mm	lingual	172.4804
6	2 mm	buccal	246.0806	6	2 mm	lingual	241.0106
7	2 mm	buccal	235.4751	7	2 mm	lingual	167.2459
8	2 mm	buccal	238.7988	8	2 mm	lingual	179.4704
9	2 mm	buccal	238.2892	9	2 mm	lingual	182.7078
10	2 mm	buccal	317.3239	10	2 mm	lingual	216.2184

15. Table of data deflection: 10-degree cusp inclination, 6-mm occlusal table dimension, with an axial loading of 250 N

Table 15

Test	Position of loading	Side of deflection on bone model	Maximum strain	Test	Position of loading	Side of deflection on bone model	Maximum strain
1	central	buccal	194.3784	1	central	lingual	215.6719
2	central	buccal	167.9899	2	central	lingual	98.44603
3	central	buccal	174.134	3	central	lingual	61.95218
4	central	buccal	178.3621	4	central	lingual	30.39357
5	central	buccal	169.4193	5	central	lingual	63.65362
6	central	buccal	134.4066	6	central	lingual	179.7765
7	central	buccal	153.8041	7	central	lingual	125.6734
8	central	buccal	166.9328	8	central	lingual	117.1885
9	central	buccal	129.8316	9	central	lingual	140.8348
10	central	buccal	139.2923	10	central	lingual	140.2502
1	2 mm	buccal	337.449	1	2 mm	lingual	330.397
2	2 mm	buccal	318.4696	2	2 mm	lingual	212.624
3	2 mm	buccal	315.591	3	2 mm	lingual	206.1445
4	2 mm	buccal	316.7544	4	2 mm	lingual	196.5215
5	2 mm	buccal	327.5916	5	2 mm	lingual	210.1628
6	2 mm	buccal	323.6991	6	2 mm	lingual	290.6224
7	2 mm	buccal	283.9579	7	2 mm	lingual	193.1713
8	2 mm	buccal	314.1869	8	2 mm	lingual	228.5458
9	2 mm	buccal	313.2115	9	2 mm	lingual	231.3364
10	2 mm	buccal	317.3239	10	2 mm	lingual	216.2184

16. Table of data deflection: 10-degree cusp inclination, 3-mm occlusal table dimension, with an axial loading of 50 N

Table 16

Test	Position of loading	Side of deflection on bone model	Maximum strain	Test	Position of loading	Side of deflection on bone model	Maximum strain
1	central	buccal	26.92162	1	central	lingual	0.007908
2	central	buccal	48.61857	2	central	lingual	34.22217
3	central	buccal	51.19623	3	central	lingual	37.24262
4	central	buccal	75.63054	4	central	lingual	64.96397
5	central	buccal	71.25787	5	central	lingual	57.68301
6	central	buccal	99.71766	6	central	lingual	93.35236
7	central	buccal	105.4012	7	central	lingual	98.82588
8	central	buccal	100.5865	8	central	lingual	91.18581
9	central	buccal	110.4665	9	central	lingual	87.57962
10	central	buccal	105.367	10	central	lingual	90.73044
1	2 mm	buccal	43.80308	1	2 mm	lingual	58.27671
2	2 mm	buccal	4.956659	2	2 mm	lingual	62.36054
3	2 mm	buccal	5.310507	3	2 mm	lingual	43.66121
4	2 mm	buccal	5.576786	4	2 mm	lingual	42.51997
5	2 mm	buccal	42.84366	5	2 mm	lingual	41.65433
6	2 mm	buccal	3.629647	6	2 mm	lingual	41.12076
7	2 mm	buccal	4.579099	7	2 mm	lingual	42.87662
8	2 mm	buccal	6.230657	8	2 mm	lingual	1.825286
9	2 mm	buccal	5.388349	9	2 mm	lingual	9.664132
10	2 mm	buccal	42.08874	10	2 mm	lingual	25.05441

17. Table of data deflection: 10-degree cusp inclination, 3-mm occlusal table dimension, with an axial loading of 100 N

Table 17

Test	Position of loading	Side of deflection on bone model	Maximum strain	Test	Position of loading	Side of deflection on bone model	Maximum strain
1	central	buccal	70.09691	1	central	lingual	11.73406
2	central	buccal	102.2772	2	central	lingual	52.71972
3	central	buccal	109.2866	3	central	lingual	57.09916
4	central	buccal	138.3644	4	central	lingual	93.60872
5	central	buccal	137.5457	5	central	lingual	79.66669
6	central	buccal	165.7085	6	central	lingual	121.8154
7	central	buccal	182.2718	7	central	lingual	135.05
8	central	buccal	191.5559	8	central	lingual	140.1257
9	central	buccal	206.53	9	central	lingual	145.2213
10	central	buccal	207.408	10	central	lingual	153.2414
1	2 mm	buccal	33.20558	1	2 mm	lingual	92.17764
2	2 mm	buccal	32.66279	2	2 mm	lingual	96.10852
3	2 mm	buccal	31.3629	3	2 mm	lingual	78.23536
4	2 mm	buccal	34.0423	4	2 mm	lingual	72.72267
5	2 mm	buccal	29.45084	5	2 mm	lingual	75.86263
6	2 mm	buccal	32.97654	6	2 mm	lingual	76.70038
7	2 mm	buccal	37.13288	7	2 mm	lingual	72.07016
8	2 mm	buccal	96.63381	8	2 mm	lingual	-1.73184
9	2 mm	buccal	102.9252	9	2 mm	lingual	-0.51362
10	2 mm	buccal	104.667	10	2 mm	lingual	-4.83757

18. Table of data deflection: 10-degree cusp inclination, 3-mm occlusal table dimension, with an axial loading of 150 N

Table 18

Test	Position of loading	Side of deflection on bone model	Maximum strain	Test	Position of loading	Side of deflection on bone model	Maximum strain
1	central	buccal	127.4653	1	central	lingual	33.82289
2	central	buccal	166.2529	2	central	lingual	74.3782
3	central	buccal	161.2559	3	central	lingual	72.05496
4	central	buccal	209.4549	4	central	lingual	111.4031
5	central	buccal	201.9346	5	central	lingual	104.7312
6	central	buccal	233.0641	6	central	lingual	145.0345
7	central	buccal	265.0687	7	central	lingual	174.3478
8	central	buccal	284.7279	8	central	lingual	189.5142
9	central	buccal	309.1028	9	central	lingual	202.691
10	central	buccal	312.3597	10	central	lingual	209.7434
1	2 mm	buccal	68.13944	1	2 mm	lingual	119.6272
2	2 mm	buccal	68.32569	2	2 mm	lingual	129.8182
3	2 mm	buccal	66.53937	3	2 mm	lingual	108.6203
4	2 mm	buccal	68.17197	4	2 mm	lingual	100.1763
5	2 mm	buccal	69.51419	5	2 mm	lingual	105.9487
6	2 mm	buccal	68.01782	6	2 mm	lingual	110.5824
7	2 mm	buccal	73.23755	7	2 mm	lingual	100.5654
8	2 mm	buccal	161.6221	8	2 mm	lingual	-13.1648
9	2 mm	buccal	171.0028	9	2 mm	lingual	-16.0531
10	2 mm	buccal	167.9649	10	2 mm	lingual	-24.3068

19. Table of data deflection: 10-degree cusp inclination, 3-mm occlusal table dimension, with an axial loading of 200 N

Table 19

Test	Position of loading	Side of deflection on bone model	Maximum strain	Test	Position of loading	Side of deflection on bone model	Maximum strain
1	central	buccal	198.8299	1	central	lingual	50.15331
2	central	buccal	227.3523	2	central	lingual	94.55924
3	central	buccal	223.2993	3	central	lingual	88.81412
4	central	buccal	274.4073	4	central	lingual	131.5158
5	central	buccal	260.6311	5	central	lingual	120.2969
6	central	buccal	297.56	6	central	lingual	157.1654
7	central	buccal	332.9653	7	central	lingual	200.7451
8	central	buccal	451.844	8	central	lingual	256.6728
9	central	buccal	394.2189	9	central	lingual	247.1934
10	central	buccal	407.2072	10	central	lingual	254.4447
1	2 mm	buccal	111.0163	1	2 mm	lingual	168.6649
2	2 mm	buccal	109.2868	2	2 mm	lingual	162.562
3	2 mm	buccal	112.8195	3	2 mm	lingual	143.48
4	2 mm	buccal	112.2489	4	2 mm	lingual	130.0398
5	2 mm	buccal	114.3455	5	2 mm	lingual	137.4288
6	2 mm	buccal	109.0496	6	2 mm	lingual	139.5976
7	2 mm	buccal	119.2608	7	2 mm	lingual	132.2106
8	2 mm	buccal	231.5951	8	2 mm	lingual	-24.2993
9	2 mm	buccal	238.9752	9	2 mm	lingual	-24.9645
10	2 mm	buccal	234.4078	10	2 mm	lingual	-29.3562

20. Table of data deflection: 10-degree cusp inclination, 3-mm occlusal table dimension, with an axial loading of 250 N

Table 20

Test	Position of loading	Side of deflection on bone model	Maximum strain	Test	Position of loading	Side of deflection on bone model	Maximum strain
1	central	buccal	325.1401	1	central	lingual	144.9971
2	central	buccal	338.7157	2	central	lingual	160.2002
3	central	buccal	335.7212	3	central	lingual	156.1105
4	central	buccal	347.8865	4	central	lingual	160.6881
5	central	buccal	327.9245	5	central	lingual	136.9312
6	central	buccal	408.8859	6	central	lingual	221.7114
7	central	buccal	431.3319	7	central	lingual	247.1553
8	central	buccal	451.844	8	central	lingual	256.6728
9	central	buccal	471.4983	9	central	lingual	273.1185
10	central	buccal	483.3105	10	central	lingual	281.3421
1	2 mm	buccal	155.488	1	2 mm	lingual	300.1648
2	2 mm	buccal	156.3366	2	2 mm	lingual	250.3959
3	2 mm	buccal	155.5391	3	2 mm	lingual	216.1031
4	2 mm	buccal	151.7587	4	2 mm	lingual	198.3371
5	2 mm	buccal	162.5747	5	2 mm	lingual	180.8868
6	2 mm	buccal	153.5335	6	2 mm	lingual	186.7608
7	2 mm	buccal	163.6545	7	2 mm	lingual	168.0915
8	2 mm	buccal	326.9997	8	2 mm	lingual	-6.79073
9	2 mm	buccal	317.421	9	2 mm	lingual	-0.31397
10	2 mm	buccal	327.7454	10	2 mm	lingual	-16.2087

REFERENCES

Aranyarachkul P, Caruso J, Gantes B, Schulz E, Riggs M, Dus I, Yamada JM and Crigger M. Bone density assessment of dental implant sites: 2 Quantity cone-beam computerized tomography. Int J Oral Maxillofac Implants 2005; 20: 416-424.

Bahat O and Handelsman M. Use of wide implants and double implants in the posterior jaw: A clinical report. Int J Oral Maxillofac Implants 1996; 11: 379-386.

Balshi TJ. An Analysis and Management of Fractured Implants: A clinical report. Int J Oral Maxillofac Implants 1996; 11: 660-666.

Berglundh T, Persson L and Klinge B. A systematic review of the incidence of biological and technical complications in implant dentistry reported in prospective longitudinal studies of at least 5 years. J Clin Periodontol 2002; 29 (suppl. 3):197-212.

Brånemark P-I. Osseointegrated implants in the treatment of the edentulous Jaw. experience from a 10-year period. Almqvist & Wiksell International. Stockholm. 1977.

Branemark PI, Adell R, Breine U, Hansson BO, Lindstrom J and Ohlsson A. Intra-osseous anchorage of dental prostheses. I. Experimental studies. Scand J Plast Reconstr Surg 1969; 3: 81-100.

Brånemark P-I, Zarb G and Albrektsson T. Tissue integrated prostheses. Chicago: Quintessence, 1985.

Brunski JB. Biomaterials and biomechanics of oral and maxillofacial implants: current status and future developments. Int J Oral Maxillofac Implants 2000; 15: 15-46.

Bryant SR. The effects of age, jaw site, and bone condition on oral implant outcomes. Int J Prosthodont 1998; 11: 470-490.

Christensen FT. Mandibular free end denture. J Prosthet Dent 1962; 12:111.

Ciberka RM, Razzoog ME, Lang BR, Stohler CS. Determining the force absorption quotient for restorative materials used in implant occlusal surfaces. J Prosthet Dent 1992; 67: 361-364.

Craig R, ed. Restorative dental materials. 6th Ed. St Louis: Mosby 1980: 60-61.

Craig R, ed. Restorative dental materials. 7th Ed. St Louis: Mosby 1985: 80.

Curtis DA, Sharma A, Finzen FC and Kao RT. Occlusal considerations for implant restorations in the partially edentulous patient. Calif Dent Assoc J 2000; 28: 771-779.

Duyck J, Ronold HJ, Van Oosterwyck H, Naert I, Vander Sloten J and Ellingsen JE. The influence of static and dynamic loading on marginal bone reactions around osseointegrated implants: an animal experimental study. Clin Oral Impl Res 2001; 12: 207-218.

Duyck J, Oosterwyck VH, Vander Stolen J, De Cooman M, Puers M and Naert I. Magnitude and distribution of occlusal forces on oral implants supporting fixed prostheses: an in vivo study. Clin Oral Impl Res 2000; 11: 465-475.

Eskitascioglu G, Usumez A, Sevimay M, Soykan E and Unsal E. The influence of occlusal loading location on stresses transferred to implant-supported prostheses and supporting bone: a three-dimensional finite element study. J Prosthet Dent 2004; 91:144-50.

Forst HM. Perspective: bone's mechanical usage windows. Bone and Mineral 1992; 19: 257-271.

Forst HM. A 2003 update of bone physiology and Wolff's Law for clinicians. Angle Orthodont 2004; 74: 3-15.

Friberg B, Sennerby L, Roos J and Lekholm U. Identification of bone quality in conjunction with insertion of titanium implants. A pilot study in jaw autopsy specimens. Clin Oral Impl Res 1995; 6: 213-219.

Geng JP, Tan KB and Lui GR. Apllication of finite element analysis in implant dentistry: a review of literature. J Prosthet Dent 2001; 85: 585-598.

Goodacre CJ, Bernal G, Rungcharassaeng K and Kan YJK. Clinical complications with implants and implant prostheses. J Prosthet Dent 2003; 90: 121-132.

Gotfredsen K, Berglundh T and Lindhe J. Bone reactions adjacent to titanium implants subjected to static load of different duration. A study in the dog (III). Clin Oral Impl Res 2001a; 12: 552-558.

Gotfredsen K, Berglundh T and Lindhe J. Bone reactions adjacent to titanium implants subjected to static load. A study in the dog (I). Clin Oral Impl Res 2001b; 12: 1-8.

Gotfredsen K, Berglundh T and Lindhe J. Bone reactions adjacent to titanium implants with different surface characteristics subjected to static load. A study in the dog (II). Clin Oral Impl Res 2001c; 12: 196-201.

Gotfredsen K, Berglundh T and Lindhe J. Bone reactions at implants subjected to experimental peri-implantitis and static load. A study in the dog. J of Clin Periodontol 2002; 29:144-151.

Guichet DL, Yoshinobu D and Caputo A. Effect of splinting and interproximal tightness on load transfer by implant restorations. J Prosthet Dent 2002; 87: 528-534.

Heitz-Mayfield L, Schmid B, Weigel C, Gerber S, Bosshardt DD, Jonsson J and Lang NP. Does excessive occlusal load affect osseointegration? An experimental study in the dog. Clin Oral Impl Res 2004; 15: 259-268.

Hibbeler RC. Mechanics of materials, 5th Ed. New Jersey: Pearson Education, Inc., 2003.

Iqbal MK and Kim S. For teeth required endodontic treatment, what are the differences in outcomes of restored endodontically treated teeth compared to implant-supported restorations? Int J Oral Maxillofac Implants 2007; 22 (suppl.): 96-116.

Isidor F. Loss of osseointegration caused by occlusal load of oral implants. a clinical and radiographical study in monkeys. Clin Oral Impl Res 1996; 7: 143-152.

Isidor F. Histological evaluation of peri-implant bone at implants subjected to occlusal load or plaque accumulation. Clin Oral Impl Res 1997; 8:1-9.

Isidor F. Influences of forces on peri-implant bone. Clin Oral Imp Res 2006; 17(suppl.2): 8-18.

Kaukinen JA, DDS, Edge MJ and Lang BR. The influence of occlusal design on simulated masticatory forces transferred to implant-retained prostheses and supporting bone. J Prosthet Dent 1996; 76: 50-5.

Khamis MM, Zaki HS and Rudy TE. A comparison of the effect of different occlusal forms in mandibular implant overdentures. J Prosthet Dent 1998; 79: 422-429.

Kim Y, Oh T, Misch CE and Wang H. Occlusal considerations in implant therapy: clinical guidelines with biomechanical rationale. Clin Oral Impl Res 2005; 16: 26-35.

Kinni ME, Hokama SN and Capto AA. Force transfer by osseointegration implant devices. Int J Oral Maxillofac Implants 1987; 2: 11-14.

Klineberg I, Kingston D and Murray G. The bases for using a particular occlusal design in tooth and implant-borne reconstructions and complete dentures. Clin Oral Impl Res 2007;18 (Suppl.3): 151-167.

Lekholm U and Zarb GA. Patient selection and preparation. In: branemark P-I, Zarb GA, Albrektsson T, ed. Tissue-integrated Prostheses: Osseointegration in clinical dentistry. Chicago: Quintessence 1985; 199-209.

Lindh T, Gunne J, Tillberg A and Molin M. A meta-analysis of implants in partial edentulism. Clin Oral Impl Res 1998; 9: 80-90.

Marx RE and Garg AK. Bone structure, metabolism, and physiology: its impact on dental implantology. Implant Dent 1998; 7: 267-276.

McAlarney ME and Stavropoulos DN. Determination of cantilever length-anterior-posterior spread ratio assuming failure criteria to be the compromise of the prosthesis retaining screw-prosthesis joint. Int J Oral Maxillofac Implants 1996; 11: 331-339.

Misch CE. Progressive bone loading. In: Misch CE, ed. Contemporary Implant Dentistry. St Louis: Mosby 1999: 595-608.

Misch CE, Susuki JB, Misch-Dietsh FM and Bidez MW. A positive correlation between occlusal trauma and peri-implant bone loss: literature support. Impl Dent 2005; 14: 108-116.

Morneburg TR and Pröschel PA. In vivo forces on implants influenced by occlusal scheme and food consistency. Int J Prosthodont 2003; 16: 481-486.

Naert IE, Duyck JA, Hosny MM, Quirynen M and Van steenberghe D. Freestanding and tooth-implant connected prostheses in the treatment of partially edentulous patients. Part I: an up to 15-years clinical evaluation. Clin Oral Imp Res 2001a; 12: 237-244.

Naert IE, Duyck JA, Hosny MM, Quirynen M and Van steenberghe D. Freestanding and tooth-implant connected prostheses in the treatment of partially edentulous patients Part II: an up to 15-years radiographic evaluation. Clin Oral Imp Res 2001b; 12: 245-251.

Norton MR and Gamble C. Bone classification: an objective scale of bone density using the computerized tomography scan. Clin Oral Impl Res 2001; 12: 79-84.

Phillips R. Science of dental materials, HBJ International Edition. WB Saunders 1990: 57-59.

Pjetursson BE, Brägger U, Lang NP and Zwahlen M. Comparison of survival and complication rates of tooth-supported fixed dental prostheses (FDPs) and implant-supported FDPs and single crowns (SCs). Clin Oral Impl Res 2007; 18 (suppl.3): 97-113.

Pröschel PA and Morneburg T. Task-dependence of activity/bite-force relations and its impact on estimation of chewing force from EMG. J of Dent Res 2002; 81: 464-468.

Rangert BR, Sullivan RM and Jemt TM. Load factor control in the posterior partially edentulous segment. Int J Oral Maxillofac Implants 1997: 12: 360-370.

Rangert B, Krogh PHJ, Langer B and Van Roekel N. Bending Overload and Implant Fracture: A Retrospective Clinical Analysis. Int J Oral Maxillofac Implants 1995:10:3:326-333.

Robert EM and Arun KG. Bone structure, metabolism, and physiology: its impact on dental implantology. Impl Dent 1998; 7: 267-276.

Richter E-J. In vivo vertical forces on implants. Int J Oral Maxillofac Implants 1995; 10: 99-107.

Salinas TJ and Eckert SE. In patients requiring single-tooth replacement, what are the outcomes of implant- as compared to tooth-supported restorations? Int J Oral Maxillofac Implants 2007; 22 (suppl.): 71-95.

Schwarz MS. Mechanical complications of dental implants. Clin Oral Impl Res II 2000; 11 (suppl.1): 156-158.

Sennerby L, Wennerberg A and Pasop F. A new microtomographic technique for non-invasive evaluation of the bone structure around implants. Clin Oral Impl Res 2001; 12: 91-94.

Sevimay M, Turhan F, Kilicarslan MA and Eskitascioglu G. Three-dimensional finite element analysis of the effect of different bone quality on stress distribution in an implant-supported crown. J Prosthet Dent 2005; 93: 227 – 234.

Smet ED, Jaecques SN, Jansen JJ, Walboomers F, Sloten JV, Naert IE. Effect of strain at low-frequency loading on peri-implant bone (re)modelling: a guinea-pig experimental study. Clin Oral Impl Res 2008; 19: 733–739.

Stanford CM. Issues and considerations in dental implant occlusion: what do we know, and what do we need to find out?. Calif Dent Assoc J 2005; 3: 329-336.

Taylor TD and Agar JR. Twenty years of progress in implant prosthodontics. J Prosthet Dent 2002; 88: 89-95.

Taylor TD, Agar JR and Vogiatzi T. Implant prosthodontics: current perspective and future directions. Int J Oral Maxillofac Implants 2000; 15: 66-75.

Tesk JA and Widera O. Stress distribution in bone arising from loading on endosteal dental implants. J Biomed Mat Res 1973; 7: 251-261.

Ulm CW, Solar P,Blahout R, Matejka M and Gruber H. Reduction of the compact and cancellous bone substances of the edentulous mandible caused by resorption. Oral Surg Oral Med Oral Pathol 1992; 74: 131-136.

Walton JN and MacEntee MI. Problems with prostheses on implants: a retrospective study. J Prosthet dent 1994; 71: 283-288.

Wang JS and Stohler CS. Textural properties of food used in studies of mastication. J Dent Res 1990; 69:1546-1550.

Wang T-M, Leu L-J, Wang J-S and Lin L-D. Effects of prosthesis materials and prosthesis splinting on peri-implant bone stress around implants in poor-quality bone: a numerical analysis. Int J Oral Maxillofac Implants 2002; 17: 231-237.

Weinberg LA. Reduction of implant loading using a modified centric occlusal anatomy. Int J Prosthodont 1998; 11: 55-69.

Weinberg LA. Therapeutic biomechanics concepts and clinical procedures to reduce implant loading. Part I. J of Oral Implantol 2001; XXVII: 293-301.

Weinberg LA. Therapeutic biomechanics concepts and clinical procedures to reduce implant loading. Part II: therapeutic differential loading. J of Oral Implantol 2001; XXVII: 302-310.

Wood MR and Vermilyea SG. A review of selected dental literature on evidence-based treatment planning for dental implants: report of the committee on research in fixed prosthodontic of the academic of fixed prosthdontics. J Prosthet Dent 2004; 92: 447-462.